

Learning from Friends in a Pandemic: Social Networks and the Macroeconomic Response of Consumption

Christos A. Makridis and Tao Wang *

April 17, 2021

Abstract

This paper studies how local shocks can have aggregate effects through the effects of social networks on expectations. First, using plausibly exogenous variation in the exposure of counties to COVID-19 shocks in their social network, we find that a 10% rise in SCI-weighted cases and deaths is associated with a 0.15% and 0.42% decline in consumption expenditures. These effects are concentrated among consumer goods & services that rely more on social-contact and are not driven by local shocks. Second, we augment a quantitative pandemic-consumption model under incomplete market with a tractable mechanism of belief formation through social communications. The model is general enough to nest a number of workhorse theories of expectation formations featuring overreaction, rational updating, or stickiness. We find that, while social communication slows the speed of aggregate belief adjustment in responses to fundamentally relevant shocks, it also moderates overreaction to local noises in aggregation. We demonstrate how the dynamic and average size of aggregate responses depend on the location of the initial shocks and the structure of the network.

Keywords: Aggregate Demand, Consumption, Coronavirus, COVID-19, Expectations, Peer Effects, Social Networks

JEL Codes: D14, E21, E71, G51

*Christos: Arizona State University, MIT Sloan, christos.a.makridis@gmail.com; Tao: John Hopkins University, twang80@jhu.edu. We would like to thank Safegraph, Facteus and Facebook (especially Mike Bailey) for providing the access to the data used in this paper. We also thank Nick Bloom, Chris Carroll, Laura Veldkamp, Johannes Stroebel, and Jonathan Wright for comments. These views are our own and do not reflect those of any affiliated institutions.

1 Introduction

The ongoing COVID-19 pandemic represents the largest world-wide shock in at least a century, leading to substantial declines in employment (Coibion et al., 2020a; Bartik et al., 2020; Cajner et al., 2020), consumption (Baker et al., 2020b; Coibion et al., 2020b), and output (Makridis and Hartley, 2020; Guerrieri et al., 2020) that surpass even the Great Recession. The vast majority of empirical contributions thus far have focused on the direct effects of the first moment shocks associated with the virus and the resulting national and state quarantine policies.¹

Using the pandemic as a natural experiment, we identify the effects of social networks on economic expectation and their macroeconomic consequences. Since social media is now a primary vehicle for obtaining information in the average household (Westerman et al., 2014), and 74% of individuals view social media as important for staying connected during the pandemic (Ritter, 2020), individuals may adjust their consumption in response to information communicated through friends in connected regions even if their own county has fairly low exposure to the virus. Quantifying how individuals make consumption and savings decisions in response to shocks to not only their fundamentals, but also those of their connected friends is important for understanding the sources of aggregate fluctuations, particularly during episodes of uncertainty and panic.

Such a question is related to a generally interesting inquiry in economics: how are individuals' decisions affected by social influences? Identifying these interpersonal influences on economic decisions is usually challenging in empirical research due to the "reflection problem" (Manski, 1993, 2000). This paper tackles this challenge by exploiting plausibly exogenous variation in individuals' exposure to COVID-19 infections in geographically remote, but socially connected, counties that vary in their friendship formed prior to the pandemic. In other words, do people adjust their con-

¹See Baker et al. (2020a) for an exception.

sumption more if they had more friends living in regions with severe epidemics? Another advantage of our approach is that it allows us to distinguish the “expectation channel” from the “preference channel” where individuals adjust their consumption based on the social norms and influences of their peers (Heffetz, 2011; De Giorgi et al., 2020). Since we exploit variation in geographically distant social connections that are identified from social network data, we believe that the effects identified here are more likely through expectations rather than preference dependence.

Using a combination of US micro card transaction data of 5.18 million consumers from Facteus and the Social Connectedness Index (SCI) from Facebook, this paper quantifies the elasticity of the individual consumption and the composition of consumption in response to the fluctuations of infections in connected counties. We find that a 10% increase in SCI-weighted cases and deaths is associated with a 0.18% and 0.23% decline in consumption, respectively. We also find that these declines are greater among social-contact-based consumption categories and activities away from home. For instance, each 10% increase in SCI-weighted cases is associated with a 0.5% decrease in clothing, footwear, cosmetics, a 1.1% decrease in contract-based service, and a 1.2% decrease in travel. These decreases are two-to-three times as large as the drop in average spending.²

We investigate the mechanisms and show that our results are not driven by time-varying shocks that are also correlated with infections in connected counties. First, we control for state \times day fixed effects, which isolates variation across counties in the same state. Furthermore, we show that increases in SCI-weighted infections are associated with stronger declines in consumption when stay-at-home orders are in place. This is consistent with the idea that social networks are more influential when consumers are unable to gather information through their personal experience around their city. Second, we conduct a wide array of heterogeneity exercises, showing that the heterogeneous treatment effects align with theory (e.g., greater effect in younger counties since social networks are

²This finding provides direct evidence for the uneven impacts of the pandemic on different sectors, which, augmented with market incompleteness, could result in a permanent drop in aggregate demand (Guerrieri et al., 2020).

more prevalent with millennials). Finally, we exploit counties' heterogeneous exposure to day-to-day changes in infections across South Korea, Italy, France, and Spain. We find similar results even when we restrict our sample to days between February 15th and March 15th 2020 prior to the U.S. national pandemic response, suggesting that our results reflect an information-driven response.

Motivated by these empirical results, this paper also makes a theoretical contribution to the literature on macroeconomic expectation formation by constructing a tractable model of social-network-based learning in which agents both privately learn from respective local news and communicate their posterior beliefs about an aggregate hidden state via a network. The model combines both efficient or non-efficient individual learning, ranging from diagnostic expectations (Bordalo et al., 2020) to information rigidity (Coibion and Gorodnichenko, 2015a) with “naive learning” (DeGroot, 1974; DeMarzo et al., 2003). Naive learning assumes that individuals’ partial belief updating is a weighted average of their friends’ posteriors and the relative weights are governed by the strength of the interpersonal ties. Due to asymmetric influences of different agents in the network, naive learning introduces additional inefficiency to the information aggregation. In such an environment, the belief dynamics and responses to shocks crucially depend on the interaction of the degree of individual responsiveness to the news and the degree of social communication. In the case of over-reaction to local news and irrelevant noises, higher social communication plays a role of a buffer that moderates belief swings. However, a higher degree of social communication also slows down the speed of belief adjustment in the face of fundamentally relevant shocks.

We then build the social-communication mechanism into a pandemic-augmented quantitative consumption model featuring market incompleteness. We assume that individuals learn about the imperfectly observable aggregate transmission of the COVID-19 via changes in local infections and then communicate their beliefs via a network, reflecting the gradual spread of information and beliefs over the course of the pandemic. Meanwhile, local infections also negatively affect income and

preferences toward the contact-based consumption. Our model not only allows us to recover belief parameters, but also provides a laboratory to explore macroeconomic counterfactual experiments. For instance, what would have been the aggregate consumption responses to infections that hit different locations or under a different network, i.e. the Facebook world in 2016?

Given a reasonable calibration to match the pre-pandemic cross-sectional consumption inequality and an externally estimated dynamics of infection, our model generates economically significant impacts of the social network on the consumption responses. For instance, following a one-time 10% increase in local infections the top one-third “influencers” in the economy, a medium degree of social communication—which corresponds to half weight to social influence—moderated the initial cut in spending by 0.5 percentage points compared to the scenario of zero social communication. This is economically meaningful: the responses imply a 5 percentage point difference to a standard permanent shock to the income. Our results also help explain the slow recovery of consumption due to the stickiness of social communication. Finally, the observed behavior of consumption cannot be explained by changes in the social network between 2016 and 2019. In sum, our model shows how social networks can amplify and propagate the effects of macroeconomic shocks.

1.1 Related Literature

The most closely related strand of the literature of this paper includes a series of studies that document the effects of online social networks on a wide range of economic decisions based on large-scale network data, especially the SCI from Facebook ([Bailey et al., 2018a,b; Makridis, 2020](#)). Different from the large body of work on peer-effects via preference dependence, this new literature particularly emphasized the role of influence channeled via expectations/beliefs, although direct evidence using belief data remains rare. Our empirical results show similar effects as these studies,

but we take one step further to build a model of belief formation reflecting social influences and apply it to a macroeconomic setting. We show it has important implications on the macroeconomic response and dynamics following shocks. We believe the model provides a handy framework to incorporate social-network-based learning in different macroeconomic settings such as the housing market, where social communication has a large role to play in driving aggregate beliefs in the presence of local and aggregate news (Burnside et al., 2016; Bayer et al., 2021).

Our work is related to a line of theoretical work on social learning that mostly focuses on equilibrium and asymptotic properties like the naive learning originally formulated by DeGroot (1974), Friedkin and Johnsen (1999) and DeMarzo et al. (2003). Further extensions of these models also explores the existence of “wisdom of crowds” (Golub and Jackson, 2010) and the spread of mis-information (Acemoglu et al., 2010). Our model modifies their formulation into a dynamic setting with newly arriving signals used for private updating. More importantly, our focuses are on dynamics and responses to local and aggregate shocks and how it is translated into aggregate belief changes and outcomes instead of long-run properties. We think this is more relevant to macroeconomic shock propagation mechanisms.

Besides, our paper directly contributes to a large literature on the household response of consumption to macroeconomic shocks, which focuses on the impact of income volatility and borrowing constraints (Zeldes, 1989; Pistaferri, 2001; Gourinchas and Parker, 2002), stimulus (Di Maggio et al., 2017; Fuster et al., 2018), tax rebates (Souleles, 1999; Johnson et al., 2006; Agarwal et al., 2007), sentiment(Carroll et al., 1994; Gillitzer and Prasad, 2018) on consumption. Quantifying how shocks affect consumption is important for understanding the presence of partial insurance and the pass-through of shocks (Blundell et al., 2008; Kaplan and Violante, 2010, 2014; Heathcote et al., 2014).³

Our results highlight the central role of social communication and information spreading of these

³See Jappelli and Pistaferri (2010) for a survey.

shocks given more realistic setting of imperfect information and individual over(under)reactions.

Finally, our paper is related to an emerging empirical literature on the role of personal experience in expectation formation. Studies have highlighted the role of personal experience in forming beliefs about future returns (Cogley and Sargent, 2008), inflation (Malmendier and Nagel, 2016; Coibion and Gorodnichenko, 2015b), energy prices (Binder and Makridis, 2020), housing prices (Kuchler and Zafar, 2019), macroeconomic activity (Malmendier and Nagel, 2011; Makridis, 2020; Makridis and McGuire, 2020), asset prices (Malmendier et al., 2018), political preferences (Giuliano and Spilimbergo, 2014), and consumption (Malmendier and Shen, 2018). Our evidence on social communications corroborates to this literature as well, as essentially communications are part of the experiences and it is fair to conjecture that the effects of experiences on expectations are by and large reinforced via interpersonal communications. This is reminiscent of models of macroeconomic expectation formation of average households via inter-personal communications (Carroll, 2003).

The structure of the paper is as follows. Section 2 describes our data and measurement approach. Section 3 presents reduced-form evidence linking SCI-weighted infections and deaths on consumption. Section 4 introduces a framework of belief formation incorporating the social learning mechanism and explores its implications for the aggregate belief responses to shocks. Section 5 extends the learning mechanism into a pandemic-augmented consumption model and calibrates it. Section 6 conducts a variety of experiments based on the model. Section 7 concludes.

2 Data and Measurement

The transaction-level data is provided by Safegraph and Facteus based on an anonymized panel of roughly 5.18 million debit card users' daily spending records between January 1st, 2017 to June 30th, 2020. Transactions are collected from primarily four types of cards providers across the United

States: (1) bank debit cards whose majority users are young people, (2) general-purpose debit cards that are primarily distributed by merchants and retailers, (3) payroll cards used between employers and employees, and (4) government cards. Average nationwide daily spending of the whole sample is 194 million dollars from a total of 2.3 million transactions.

Three features make the data particularly useful to our analysis.⁴ First, there is rich geographic heterogeneity. In particular, transactions are partitioned by the residential zipcode of the card user. We then aggregate zip-level transactions into county-level consumption observations of 3051 counties (out of 3141 in the United States as of 2019). For zip zones that are associated with multiple counties, we allocate total consumption to its multiple corresponding counties based on its population weights. To ensure the county-level consumption is not biased by abnormal individual users' records and extreme values, we restrict our sample to include only county-day observations with more than 30 card users. Daily average consumption expenditures per card user is roughly \$40 based on 0.5 transactions.

Second, there is high-frequency variation. In particular, we exploit the daily variation in transactions to identify the response of consumption to news about the pandemic. Since the epidemic crisis has eclipsed nearly ever other national and international event with release of daily news on the number of infections and deaths, daily records provide much cleaner variation than the common alternative of monthly data to recover the effects of news and social media. Although the transaction data goes back to 2017, we restrict the sample to the period between February 1st and June 30th with a total of 152 days and roughly 450,000 county \times day observations. This period spans from the early spreading stage of the COVID-19 in Asian and European continents to the peak of

⁴However, one limitation of our data is that the location of a transaction differs from the location of residence; we only observe the latter. While we suspect that exploiting county-level (rather than zipcode-level) variation mitigates this concern, since people consume locally most of the time, we view potential misclassification as a source of measurement error (Chen et al., 2011). This would bias us against finding a result. We nonetheless conduct robustness where we investigate potential heterogeneous treatment effects in areas that have high versus lower levels mobility in "normal times", i.e. college towns.

the crisis within the United States. Depending on if the focus of analysis is domestic or international, we split our sample with the cutoff date of March 15—a widely acknowledged watershed in nationwide response to the crisis in the country.

Finally, spending transaction is recorded by the merchant’s type identified by its merchant classification code (MCC), a commonly adopted classification scheme by major card providers such as Visa/Mastercard. This allows us to study the consumption responses by category. We group each one of the 982 MCCs into 16 broad categories based on its degree of exposure to the infection risks.⁵ For instance, eating/drinking/leisure outside the home, contact-based service such as barbershop, and travel are expected to be most severely hit by the infection risk. Grocery and food shopping, financial services, and housing utilities, in contrast, are expected to have mild responses to the pandemic news during this period.

Figure 1 plots the average daily spending of each month since February 2020 by consumption category. The bulk of the consumption is accounted for by goods and services that are generally most exposed to the pandemic, including eating and drinking, leisure outside of the home, contact-based services, travel and transportation, and clothing, footwear, and cosmetics. However, some goods and services, such as financial services, grocery shopping, and home leisure, have actually increased in March, relative to the two months prior. One important difference in the data, however, is that grocery shopping and other necessary purchases account for a large share in total spending, reflecting the fact that the composition of consumers in the sample is lower income and younger than a more nationally representative sample.

[INSERT FIGURE 1 HERE]

While the data contains these three important advantages over the traditional sources, we nonetheless are concerned about whether the data is nationally representative enough to map

⁵See Section A.1 in the Online Appendix for examples of merchant types that fall into each category.

elasticities identified in the micro-data to the aggregate economy. We explore several validation exercises. First, Figure 2 plots monthly total spending in contact and non-contact sectors based on our transaction records and the advanced retail sales provided by the Census Bureau. For each sector, we combine sub-category series to make the retail sales data approximately comparable with that constructed from the transactions. Specifically, the contact-based consumption for retail sales is approximated by the sum of “drinking and eating places” (RSFSDP) and “health and personal car” (RSHPCS). The non-contact consumption is approximated as the total of “grocery store” (RSGCS) and “food and beverage stores” (RSDBS).

As shown in the Figure 2, in both sectors, our separately constructed time series track with each other reasonably well, although they are not apples to apple comparisons—the correlation is 0.55 in non-contact consumption and 0.26 in contact consumption over the four-year period that overlaps.⁶ Despite the lower correlation in contact consumption, importantly, both series mark a dramatic drop in spending in March 2020 and a similar recovery since late April. In its trough, the retail sales and food service decreased by around 16.4% from the same month last year. Given our empirical analysis primarily rely upon the subsample of the year 2020, we are additionally assured about the representativeness of our results.

[INSERT FIGURE 2 HERE]

We also draw on the Social Connectedness Index (SCI) from Facebook⁷, introduced originally by Bailey et al. (2018b) to study how information about housing prices is diffused among social networks and affects the decision to rent versus own a home. This data are now used more widely

⁶Some of the differences between the two series may emerge because the sample selects lower-income individuals and does not have complete coverage throughout the country. These low income and younger groups are widely known in the literature to have a high Engel index, i.e. a large share of spending on necessities such as grocery/food. That means the composition of the spending recorded in the transaction is geared toward basic items. Moreover, both low-income and young people tend to have a high marginal propensity to consume (MPC) due to under insurance. This will undoubtedly induce more volatility in consumption spending across different periods.

⁷Till 2011, there were about 149 million users of Facebook in the U.S. out of the 260-million eligible population, 15.9 billion edges, an average of 214 friend ties per user (Ugander et al. (2011)).

to understand how social ties are related with economic activity (Bailey et al., 2018c) and expectations about macroeconomic activity (Makridis, 2020). The index is constructed from anonymized information between all Facebook users, counting the number of friendship ties between county c and every other county c' in the United States. We use the 2019 data extract. Each user is limited to a total of 5,000 friends on a profile. Network ties require that both sides agree. Finally, we obtain the number of COVID-19 infections and deaths at the county \times day level from the Center for Systems Science and Engineering from Johns Hopkins.⁸

3 Reduced-form Evidence

3.1 Identification Strategy

While several emerging papers now document a substantial drop in consumption and its composition over the course of the pandemic (Baker et al., 2020b; Coibion et al., 2020b), these studies focus on the direct effects of the national quarantine on spending patterns. However, since individual financial behaviors are also a function of peer effects (Moretti, 2011; Bursztyn et al., 2014), we investigate whether there is evidence of a decline in consumption prior to the national quarantine mediated through social networks. In particular, we draw on the Social Connectedness Index (SCI) to produce an SCI-weighted index of COVID-19 cases and deaths:

$$COVID_{ct}^{SCI} = \sum_{c' \neq c} (COVID_{c',t} \times SCI_{c,c'}) \quad (1)$$

where $COVID_{ct}^{SCI}$ denotes the logged SCI-weighted number of cases or deaths in connected counties, $COVID_{c',t}$ denotes the logged number of cases or deaths in county c' , and $SCI_{c,c'}$ denotes

⁸See Figures A.1 and A.2 in Section A.2 of the Online Appendix.

our measure of the SCI. We underscore two important features about our construction of $SCI_{c,c'}$.

First, we omit the number of friendship ties between county c and itself, thereby exploiting only the variation in its exposure to other locations. This means that Equation 1 will not “double count” local infections. Second, we normalize the number of friendship ties in a county to its total number of friendship ties, thereby exploiting the relative exposure to other locations. This means that differences in the level of friendship ties will not explain differences in consumption; only relative differences across counties.⁹ Using this SCI-weighted index of the number of cases and deaths, we consider regressions of the following form that also control for local infections:

$$y_{c,t}^k = \gamma COVID_{c,t}^{SCI} + \phi COVID_{c,t} + \zeta_c + \lambda_t + \epsilon_{c,t} \quad (2)$$

where $y_{c,t}^k$ denotes logged consumption for county c on day t for category- k consumption good, and ϕ and λ denote fixed effects on county and day-of-the-year. We cluster standard errors at the county-level to allow for arbitrary degrees of autocorrelation over time.

Our identifying variation in Equation 2 comes from the fact that the social network in a county is pre-determined with respect to the infections that it and others faces over the coronavirus pandemic. Consider, for example, two counties that share the same population, industrial and occupational composition, and education and age distributions. To the extent that they are both heterogeneously connected to different external counties, then their local response might differ as some residents hear more pessimistic versus optimistic information. We believe that the variation in heterogeneous exposure to other counties is plausibly exogenous. We also consider additional robustness exercises where we exploit the exposure of different *countries* to the pandemic based on

⁹For example, suppose that county A has 100 friendship ties with county B and county C. If county D has 1000 ties with both county B and C, then the level of friendship ties would differ, but the relative amount is the same. Because we do not want to confound differences in the level of social media and/or network exposure with consumption, but rather focus on the connectivity to different locations, we normalize our measure. However, we also obtain qualitatively similar results if we leverage the differences in levels too.

their social connectivity before the quarantines began in the United States in March 2020.

3.2 Main Results

Table 1 documents the results associated with Equation 2. We begin with a standard fixed effects estimator in columns 1 and 6, exploit variation within the same county over time. We find that a 10% rise in SCI-weighted cases and deaths are associated with a 0.51% and 0.62% decline in consumption expenditures, respectively. One concern with these results, however, is that we are failing to control for local infections and deaths. If, for example, counties that are relatively more exposed to counties with higher infections also have higher infections themselves in some time-varying way, then we may obtain downward biased coefficient estimate.

To address these concerns, columns 2 and 7 control for logged county cases and deaths. Consistent with our concerns about the potential for bias, our point estimate on the SCI-weighted infections index declines: a 10% rise in SCI-weighted cases and deaths is associated with a 0.15% and 0.42% decline in consumption expenditures respectively. Moreover, increases in contemporaneous local cases are also associated with declines in consumption, but with a lower magnitude. Local deaths also decrease consumption by a similar degree, but are statistically significant. We have also experimented with one-week and two-week lags on county cases and deaths because of the incubation period for the virus, but the results are not statistically different: if anything, the gradient on SCI-weighted cases is slightly higher.

Yet another concern is that state policies vary considerably over these months. Even though there was a national quarantine, states introduced policies of varying restrictiveness, including stay-at-home orders (SAHOs). For example, [Ali et al. \(2021\)](#) find that the adoption of SAHOs is associated with a persistent decline in job postings for early care and education. This may also

impact consumption by shifting the composition of goods and the overall amount of goods as parents stay home. Consistent with this interpretation, columns 3 and 8 show that the adoption of a SAHO is associated with a 5.6-5.8% decline in consumption. Moreover, increases in SCI-weighted cases and deaths continue to have a negative association with consumption.

Next, we exploit variation in SAHOs to provide an additional diagnostic into the potential causal interpretation of our estimates. If social networks have a causal mediating effect on consumption, then our estimates should be concentrated in states and days that have enacted SAHOs since they keep individuals in doors where they are more likely to rely on social networks for information through, for example, Facebook, rather than through personal experience. Consistent with our hypothesis, columns 4 and 9 show that a 10% rise in SCI-weighted cases and deaths following the adoption of a SAHO is associated with an additional a 0.24% and 0.26% decline in consumption expenditures, which is roughly twice the magnitude obtained in columns 2 and 7. These coefficients are also more precisely estimated, significant at the 1% level.

Finally, there could still be other time-varying shocks to consumption even after our inclusion of the time-varying state policy controls. Columns 5 and 10 introduce state \times month fixed effects, exploiting variation within a county after controlling for all shocks that are common to a given state-month pair. This pushes the data even further by purging variation in consumption that could be correlated with any state policy. We find that a 10% rise in SCI-weighted cases and deaths is associated with a 0.16% and 0.59% decline in consumption expenditures. While the coefficient for SCI-weighted cases \times SAHO is only significant at the 10% level, the coefficient for SCI-weighted deaths \times SAHO remains significant at the 1% level and even slightly higher than the baseline result in column 7. The fact that COVID-19 related deaths have a larger association with consumption expenditures than cases is intuitive since they are more salient and damaging than infections.

[INSERT TABLE 1 HERE]

How do these information shocks potentially heterogeneously affect spending across different types of consumer goods? Figure 3 documents these results by reporting the coefficients associated with major categories of goods, which we created based on merchant category codes (MCC) in the transaction data. We report the coefficients associated with both the direct effect of infections and the indirect effect through propagation from social networks. Not surprisingly, we find that clothing, footwear, and cosmetic products decline the most, followed by contact-based services, durables, travel, and eating or drinking outside the home. For example, a 10% rise in SCI-weighted infections is associated with nearly a 0.5% decline in clothing, footwear, and cosmetic spending, whereas the effects on grocery/food or home leisure spending are nearly zero. These results are consistent with Coibion et al. (2020b) who find a 31 log point drop in consumer spending concentrated in travel and clothing. Similarly, we see the largest association for contact-based consumption: a 10% rise in SCI-weighted infections is associated with a 1.3% decline in consumption.

[INSERT FIGURE 3 HERE]

3.3 Heterogeneous Treatment Effects Across Space

We now turn towards evidence of heterogeneity in the treatment effects by county characteristics. We control for the direct effects of county infections and deaths, focusing on variation in the SCI-weighted infections. We focus on per capita income, the age distribution, population, the share of digitally-intensive employees as defined by Gallipoli and Makridis (2018), and the share of teleworking employees as defined by Dingel and Neiman (2020). We partition each variable based on the median value, allowing for heterogeneity above and below the median. Our results with the digital and telework shares are both estimated on a restricted sample because we obtain them from the American Community Survey micro-data, which does not cover every county.

Table 2 documents these results. While not all the differences across different types of counties are statistically distinguishable from one another, they are consistent with theory. For example, a 10% rise in the SCI-weighted infections is associated with a 0.47% decline in consumption among the counties below the median in per capita income and a 0.12% decline among the rest. This could be consistent with the presence of greater information asymmetries in lower income counties, so individuals have to rely on more informal networks for information. However, given that our consumption data has better coverage in lower income areas, it is possible that we simply have more measurement error in higher income counties.

Turning towards heterogeneity in the age distribution, we distinguish among those counties that rank above and below the median in terms of the share of individuals below age 35 and the share of individuals above age 65. We do not see statistically different effects when we partition by the median share of individuals below the age of 35: in both cases, a 10% rise in SCI-weighted infections is associated with a 0.21-0.25% decline in consumption. However, when we partition on the median share of individuals over age 65, we find that the elasticity is concentrated in counties with lower shares, implying a 0.28% decline in consumption (compared with a 0.14% decline for counties with higher shares of individuals over the age of 65). This is consistent with the fact that younger individuals are more likely to pay attention to information from social media ([Smith and Anderson, 2018](#)). We also find that the effects are concentrated among counties with a larger population.

Finally, we do not see much of a difference between states that rank higher versus lower in terms of digital intensity ([Gallipoli and Makridis, 2018](#)), but we do see a larger elasticity for states that have a higher share of telework ([Dingel and Neiman, 2020](#)). This could be consistent with the fact that states with more remote workers are likely to rely more on social networks for information, rather than personal experience.

[INSERT TABLE 2 HERE]

3.4 Understanding the Mechanisms

We have shown that there is an economically and statistically meaningful decline in consumption associated with increases in the number of COVID-19 infections in socially connected counties even after controlling for time invariant characteristics across space and time, as well as time-varying shocks to local health outcomes (e.g., infections and deaths). However, one concern is that these results are plagued by other time-varying omitted variables that jointly affect connected counties and local consumption outcomes. This section provides further evidence that the results reflect a genuine information effect, rather than potential omitted variables.

One of the primary examples of omitted variables bias is the introduction of state-specific policies. For example, one possibility is that the introduction of emergency orders within a state naturally lead to declines in consumption by significantly disrupting foot traffic and leading to closures of businesses. While we show that our results are robust to controlling for state \times day fixed effects, we nonetheless explore this possibility further by exploiting variation in the staggered introduction of state-specific stay-at-home orders (SAHOs) using data from [Ali et al. \(2021\)](#). If, for example, the introduction of SAHOs and other state policies account for the decline in consumption ([Coibion et al., 2020b](#)), then we should see that the effect of the SCI-weighted infections loads on the interaction between it and the SAHOs. However, when we estimate these fixed effect specifications, we find a statistically insignificant point estimate of -0.002. This placebo counters the possibility that there are other unobserved and time-varying county-specific policies that vary with both consumption and connected counties.

We further investigate the role of social networks by turning towards measures of international exposure for each county, leveraging the fact that some countries began experiencing the surge in COVID-19 cases much sooner and more severely than the United States. We focus on four

countries—South Korea, Italy, Spain, and France—although our results hold on a broader set of countries exposed early on.¹⁰ Each of these four countries successively experienced large number of infections in different scale since late February preceding the United States.

We exploit variation along two dimensions. First, counties vary cross-sectionally in their exposure to these countries. For example, whereas Maricopa County in Arizona has an SCI of 142,771 with France, San Francisco has an SCI of 258,825. Second, countries vary in their intensity of COVID-19 shocks. Figure 4 shows how Italy experienced a sharper and more severe surge in cases than France even though its population is roughly 6 million smaller. We now consider regressions of logged consumption on the product of the cross-sectional exposure to a country and its time series variation in infections, conditional on the usual county and day fixed effects. Importantly, we restrict our sample to the period between February, 15th to March, 15th, which covers the time leading up to the full-scale outbreak in the United States.¹¹ This allows us to purge variation that is possibly correlated with time-varying shocks in the United States.

Table 3 documents these results. We find that there is a robust negative association between the SCI-weighted number of infections / deaths and consumption for each country. For example, a 10% rise in infections (deaths) in Italy for counties that are more closely connected to Italy is associated with a 0.07% (0.52%) decline in consumption. One reason for the potentially larger coefficient on deaths over infections stems from the way that media covers international deaths more intensively than the number of infections, although we cannot say conclusively. We see broadly similar treatment effects for each country, although they are smaller for France, perhaps because the United States had already witnessed the experience of Asian countries, like South Korea, and

¹⁰Although we would, of course, ideally include China, the Facebook data does not have representative coverage of ties with China because their government prohibits the use of Facebook.

¹¹We also conduct the same analysis for the period after March, 15th for a different consideration. Since the Federal government of the U.S. announced the travel ban from Europe in the same week, focusing on this later period potentially shuts down the channel via which socially connected cases posed a real risk of infection. The negative impacts of consumption by SCI weighted cases from each of this country, if any, becomes more significant.

Spain and Italy earlier in the month of March.¹²

[INSERT TABLE 3 HERE]

Our finding that consumption in one county depends on the infections among connected counties—even if they are geographically distant—builds directly on an emerging literature on the real effects of social connectedness (Bailey et al., 2018c,b). However, separately identifying the causal effect of shocks to a network from selection effects is challenging (Goldsmith-Pinkham and Imbens, 2013). Our diagnostics—the combination of domestic and international connectivity—suggest that we are detecting meaningful effects from social networks, rather than just selection effects, but this remains an area of ongoing research. Our paper is also related with recent evidence from Charoenwong et al. (2020) that finds some counties were more likely to adopt social distancing and restrictions measures based on their exposure to Italy and China, although the data on social connectivity to China is confounded by the fact that use of Facebook is blocked within the country.

4 A Model of Learning on the Social Network

4.1 Social Network and Listening Matrix

We implicitly consider each agent as representing a county analogous to our data and we use the terms agent, consumer, and county interchangeably. Agents are connected through a pre-determined social network: we assume away the endogenous formation of the network structure for simplicity, but the model can easily accommodate time-varying networks. Agent i is a particular node in a given social network. Nodes differ from each other ex-ante in their location of the network, as well as ex-post in its experienced idiosyncratic shocks/private signals. We denote the thickness of

¹²Section A.3 of the Online Appendix also presents additional diagnostics that mitigate concerns that our results simply reflect differences in physical distance between connected counties.

the link between any two nodes i and j , the analog to the observed SCI from the data, as $l_{i,j}$. It follows that if county i and j have no connections, $l_{i,j} = 0$. The scale of $l_{i,j}$ reflects the degree of connectedness between the two. Links are undirected, so $l_{i,j} = l_{j,i}$. We assume within each node i there is non-zero connectedness sized of $l_{i,i} = l_i$, which accounts for within-region connections.

The agents communicate their beliefs about an unobservable aggregate state across the network through connected nodes. The structure of the social connections determines the strength of the direct node-to-node influence on the information exchange. Through the whole network, these influences can be captured by a matrix W , which we refer to as the listening matrix following DeMarzo et al. (2003). This is different from the term social influence that measures cumulative influence among nodes after repeated social interactions. The i, j -th entry of the matrix W , defined as the weight given to j by i , is the number of lies i has with j as a share of total ties i has.

$$w_{i,j} = \frac{l_{i,j}}{\sum_{k=1}^N l_{i,k}} \quad (3)$$

Therefore, each row i of the matrix W reflects the influence weights that node i assigns to all of its connected nodes, including some non-zero weight $w_{i,i}$ to itself. Hence, the row sum of the matrix is always equal to 1.

$$\sum_{k=1}^N w_{i,k} = 1 \quad \forall i \quad (4)$$

Correspondingly, the column sum of the listening matrix W is what we define as the degree, following the network analysis literature. The degree of node j is a measure of how influential it is among the entire network.¹³

¹³Other studies also characterize the network structure using degree distribution, such as social learning (DeMarzo et al., 2003), output-input linkages (Acemoglu et al., 2012), investment network (Lehn and Winberry, 2019), etc.

$$d_j = \sum_i^N w_{i,j} \quad (5)$$

The interpersonal influence is not necessarily symmetric between two nodes because the weights are normalized by the node-specific social connectedness. For instance, node a may be the single connected node b has while b is just one of many by a . In addition, since the within-node link is never zero, any element in the diagonal of the matrix W is always positive and attains its maximum value of 1 when the node has zero connections with the rest of the network. W being equal to an identity matrix is the special case of social autarky where each node has only itself as a friend. W has every entry taking the value of $1/N$ is an “egalitarian” matrix where everyone has equal influence on each other, including on themselves. Both autarky and egalitarian listening matrices belong to symmetric listening matrices where the bilateral influence between two nodes is balanced.

The listening matrix constructed from the real world and to be used for our analysis in this paper is far from symmetric. We compute W using the SCI from Facebook at the county level. The number of nodes (representative consumers in the later section) is equal to the number of counties for which we have data: $N = 3141$ (see Figure A.3 in Section A.2 of the Online Appendix for the heat map corresponding to the listening matrix using 2019 SCI data). We rank counties by their FIPS code so that counties from the same state are adjacent in the graph. The diagonal blocks have greater weight indicating the dominant influence within the county. The rectangular blocks along the diagonal also have higher weight indicating stronger influence within the same state. There is substantial variation across different counties in terms of both their inward and outward influence.¹⁴

¹⁴Figure A.4 in Section A.2 of the Online Appendix plots the SCI distribution of degrees in 2016 and 2019.

4.2 Belief Updating

Agents in the network are learning about an unobservable aggregate state ψ_t (the spreading speed of the virus in our pandemic setting) via both private signals (changes in local infections) and social communications. The social learning takes the form of naive learning formulated by (DeGroot, 1974; DeMarzo et al., 2003; Golub and Jackson, 2010). Agents first update their beliefs using private signals and then communicate their posteriors with connected friends. Communication leads to partial updating of beliefs by taking a weighted average of posteriors of their friends from the previous period and the weight is proportional to the pairwise influences dictated by W .

Specifically, assuming a constant weight λ is given to social communication and the rest comes from private updating, the post-communication belief $\tilde{\psi}_{i,t}$ is a weighted sum of privately updated belief $\hat{\psi}_{i,t}$ and socially updated belief $\sum_{j=1}^N w_{i,j} \tilde{\psi}_{j,t-1}$, which is a variant of naive learning from Friedkin and Johnsen (1999). However, instead of assuming the individually updated belief to be the initial prior, we assume it to be updated each period.. λ is one of the key structural parameters in this model. A higher value of λ implies greater importance of social communication.

$$\tilde{\psi}_{i,t} = (1 - \lambda)\hat{\psi}_{i,t} + \lambda \sum_{j=1}^N w_{i,j} \tilde{\psi}_{j,t-1} \quad (6)$$

Private learning is based on a individual noisy signal $s_{i,t}$. We assume a general form of the private learning that nests different expectation formation mechanisms developed in the literature, including: Kalman filtering, constant-gain learning that nests overreaction via “diagnostic expectations” (Bordalo et al., 2020), or underreaction potentially due to inattention or information rigidity (Coibion and Gorodnichenko, 2015a). All mechanisms share a common structure: a weighted average of the post-communication prior in the previous period and the new signal.

$$\hat{\psi}_{i,t} = (1 - \kappa_{i,t})\tilde{\psi}_{i,t-1} + \kappa_{i,t}s_{i,t} \quad (7)$$

In the equation above, $\kappa_{i,t}$ is the weight given to the new information $s_{i,t}$. Alternative assumptions regarding its specific form nest different belief updating protocols. In the case of Kalman filtering, the weight is efficiently adjusted to reflect the relative precision of signals and prior uncertainty each period. The learning is known to be more efficient than other constant-gain learning algorithms under imperfect information. We can therefore consider this case as an individual rationality benchmark. Denote the steady-state gain from Kalman filtering as κ^* .

We primarily focus on the constant-gain learning in updating, believing this to be more realistic. Assuming $\kappa_{i,t}$ takes a constant value k across time and individuals. It nests alternative mechanisms seen in the literature. If $k > \kappa^*$, the belief constantly extrapolates surprises $s_{i,t} - \tilde{\psi}_{i,t-1}$, generating overreaction to the news. The degree of overreaction increases with the $k - \kappa^*$.¹⁵ $k = 1$, as a special case, represents an agent with a very fickle belief that fully reacts to the news forgetting about prior beliefs entirely. If $0 < k < \kappa^*$, the agent is attentive to the news but only partially reacts to it leaving the rest weight given to priors. This is essentially similar to an inefficient Bayesian updating. If $k = 0$, the agents entirely ignore the news and stick to their prior beliefs. This could be due to information rigidity or full inattention at the agent level. The existing literature does not provide a good theoretical foundation for the case when $k < 0$, which could arise when the agent adjusts the belief in the opposite direction to the surprises and loads more weight on their priors. We restrict the values of k to be between 0 to 1.

Regardless of the specific private learning rule, combining private and social learning defined

¹⁵For the micro foundation of belief extrapolation in an environment of noisy information, see [Bordalo et al. \(2020\)](#).

above gives a linear recursive formula expressed only in terms of post-communication belief $\tilde{\psi}_{i,t}$.

$$\tilde{\psi}_{i,t} = (1 - \lambda)(1 - k)\tilde{\psi}_{i,t-1} + \lambda \sum_{j=1}^N w_{i,j}\tilde{\psi}_{j,t-1} + (1 - \lambda)ks_{i,t} \quad (8)$$

Incorporating such social learning is “naive” for the following reason. When agents repeatedly take the average of the posteriors of their connected nodes using the constant weight, they fail to account for possible repetition in the information contained in others’ signals as if they are independent signals. This heuristic rule is justified by assuming agents do not have perfect knowledge of the whole network structure and cannot trace the source of information received from friends due to bounded rationality (Chandrasekhar et al., 2020). Instead of optimally adjusting the weights to each signal based on their precision, each person simply uses the same weights from social connectedness. This gives rise to the “persuasion bias” shown in DeMarzo et al. (2003). It states that the consensus that arises after repeated communications among agents does not converge to the correct belief unless the social influence structure is balanced. The model also implies persistent differences in opinions in the presence of heterogenous priors and the speed of belief convergence is slower than a rational framework where agents optimally adjust weights given the precision of signals.

It is also very convenient to characterize the belief dynamics of the entire society. Stacking individual beliefs into a N -sized vector $\tilde{\psi}_t$ each period after social learning, the belief dynamics can be summarized by the following.

$$\begin{aligned} \tilde{\psi}_t &= M\tilde{\psi}_{t-1} + (1 - \lambda)ks_t \\ M &= (1 - \lambda)(1 - k)I + \lambda W \end{aligned} \quad (9)$$

where s_t is a $N \times 1$ vector stacking all individual signals at t and κ_t is a $N \times N$ matrix with its i -th diagonal element being the agent i 's information gain and zeros elsewhere. I is an identity matrix sized N . The weight assigned to the previous belief M consists of one component from individual updating and another from social communication determined by the network structure W (given $\lambda > 0$). In general, M can be time-varying if we maintain Kalman-filter gain $\kappa_{i,t}$. Since we focus on constant-gain learning, the time subscript is dropped from M .

Regardless of the form of individual learning, the presence of social communication ($\lambda > 0$) introduces a potential belief amplification mechanism at the society level. To see this clearly, imagine an exogenous belief shock to the node j at time t , and denote the aggregate belief 1 period following the shock as $\tilde{\psi}_{t+1}^{av}$. The belief multiplier (MP) can be defined as the ratio of the aggregate belief between two scenarios with/without social communication.

$$MP_{t+1|t}^j = \frac{\delta\tilde{\psi}_{t+v}^{av}/\delta\tilde{\psi}_{j,t}(\lambda \neq 0)}{\delta\tilde{\psi}_{t+v}^{av}/\delta\tilde{\psi}_{j,t}(\lambda = 0)} = \left(\frac{d_j}{1-k} - 1\right)\lambda + 1 \quad (10)$$

Social communication initially amplifies the aggregate belief response to an individual's belief shock to j if $MP_{t+1|t}^j > 1$ since $\lambda > 0$, which holds when $d_j + k > 1$. This implies a higher influence in the degree of the node j or higher individual responsiveness to the news tends to amplify the local shocks to the aggregate level. Although the multiplier depends on the rounds of communication following the shock, this holds over the multiple periods (see Appendix A.4).

By the same token, we can imagine an exogenous aggregate belief shock to all nodes. And the social belief multiplier v periods after the shock is the following (See Appendix A.4 for derivations)

$$\begin{aligned}
MP_{t+v|t} &= \frac{1}{N} \sum_{j=1}^N MP_{t+v|t}^j = \Theta^v \\
\Theta &= 1 + \frac{k\lambda}{1-k}
\end{aligned} \tag{11}$$

Notice here that unlike the responses to local shocks, the responses to aggregate belief shocks do not depend on the structure of the network anymore. But the presence of social communication still leads to amplification effects. The condition for belief amplification holds, i.e. the belief multiplier is greater than 1, for any positive value of λ and k .

This has important implications for how macroeconomic shocks propagate. The belief dynamics crucially depend on the parameter values of k and λ . Another determinant of the belief dynamics in the case of local/idiosyncratic and distribution is the structure of the listening matrix. The most relevant structural property is the distribution of degrees across agents. For all balanced or symmetric listening matrices with zero-dispersion (every node has a degree of 1), the structure of the network and the location of the shocks is no longer relevant to the transmission of local shocks to aggregate beliefs. An asymmetric matrix with higher degree dispersion implies more asymmetric influences among agents and that local shocks to nodes of different influences would now have disproportionate impacts in aggregate belief and its dynamics.

5 A Quantitative Model of Consumption in the Pandemic

This section builds the network-based learning framework formulated in Section 4 into a pandemic-augmented consumption and saving model with uninsured idiosyncratic income risks and borrowing constraints. We explore whether the effect of social influences in individual expectation and consumption spending generate a sizable aggregate response that alters the macroeconomic dynamics.

We allow for two consumption sectors that are potentially affected differently by the pandemic. Moreover, given our primary focus is the propagation mechanisms of aggregate demand via social networks, we adopt a partial equilibrium approach by taking the supply side of the economy as given. However, nominal rigidity and cross-sector frictions could be added to a general equilibrium model so that the aggregate demand generates real effects in output and unemployment.

5.1 The Consumer's Problem

The economy is populated by N infinitely-lived consumers, indexed by i . Each consumer derives utility from a stream of consumption in the current and all future periods.

$$\max \quad E_0 \sum_{t=0}^{\infty} \beta^t u(c_{i,t}) \quad (12)$$

The instantaneous utility within each period takes a CRRA form with relative risk aversion ρ (and the elasticity of inter-temporal substitution $\frac{1}{\rho}$).

$$u(c) = \frac{c^{1-\rho}}{1-\rho} \quad (13)$$

Total consumption in each period, denoted as c_t , is a CES (constant elasticity of substitution) bundle of goods/service from two sectors: one contact-based represented by subscript c and non-contact-based consumption by n , respectively.

$$c_{i,t} = (\tau_{i,t} \phi_c c_{i,c,t}^{\frac{\epsilon-1}{\epsilon}} + (1 - \phi_c) c_{i,n,t}^{\frac{\epsilon-1}{\epsilon}})^{\frac{\epsilon}{\epsilon-1}} \quad (14)$$

The elasticity of substitution between two sectors is ϵ and the relative preference weight are ϕ_c and $1 - \phi_c$: a larger ϵ implies the two sectors are more substitutable and a larger ϕ_c implies a

stronger relative preference toward contact-based consumption. Moreover, the taste shock, denoted as $\tau_{i,t}$, scales the utility from contact-based consumption. In steady state, it takes a value of 1.

In each period t , the agent receives an idiosyncratic draw of the taste shock, $\tau_{i,t}$, which varies with the local infections, and this is specified later. Lower $\tau_{i,t}$ implies less utility from consuming contact-based services due to exposure to infection. This conveniently captures the idea that consuming contact-consumption bears higher health risks from the individual's point of view. A lower utility from contact-based consumption could be either due to self-precautionary actions to avoid infection or compliance of local government containment policies such as stay-at-home orders.

The inter-temporal budget and borrowing constraints of the agent i at time t are.

$$\begin{aligned} c_{i,t} + a_{i,t} &= m_{i,t} \\ m_{i,t} &= y_{i,t} + b_{i,t} \\ b_{i,t+1} &= a_{i,t}(1+r) \\ a_{i,t} &\geq 0 \end{aligned} \tag{15}$$

where $a_{i,t}$ is the end-of-period saving at a real interest rate r , $m_{i,t}$ is the total wealth in hand, consisting of the current bank balance $b_{i,t}$ and the labor income $y_{i,t}$, which is determined by.

$$\begin{aligned} y_{i,t} &= n_{i,t} o_{i,t} z_{i,t} \\ \log(o_{i,t}) &= \log(o_{i,t-1}) + v_{i,t} \\ v_{i,t} &\sim N\left(-\frac{\sigma_v^2}{2}, \sigma_v^2\right) \end{aligned} \tag{16}$$

where $n_{i,t}$ is the labor supplied inelastically, which we normalize to one. The labor income

received by individual i depends on the realizations of two multiplicative idiosyncratic income shocks: a permanent component $o_{i,t}$, and a transitory (or a persistent) component $z_{i,t}$, which is potentially a function of local infection. The logged permanent income $o_{i,t}$ follows a random walk with i.i.d. shock of size σ_v .¹⁶ The component $z_{i,t}$ is equivalent to a standard transitory income component without the impact from the local infection. During the pandemic, a higher infection will lead to a lower income or unemployment. We specify $z_{i,t}$ as a function of infection later.

5.2 The Pandemic

We model the pandemic as an agent-specific stochastic state that evolves subject to both aggregate and idiosyncratic shocks. Each agent i at time t is faced with a local infection state, $\Xi_{i,t}$, which represents the severity of the local epidemic. It could be approximated, for example, by the actual number of infected cases in the region. $\Xi_{i,t}$ grows exponentially with two multiplicative components: one being an aggregate growth rate of e^{ψ_t} , and the other being an idiosyncratic shock $e^{\eta_{i,t}}$. The combined growth rate from the two shocks is equivalent to what is commonly referred to as the “reproduction rate” in a micro-founded epidemiological model such as SIR or SIRD.¹⁷ The aggregate state follows a random walk. Both aggregate shock θ_t and idiosyncratic shock $\eta_{i,t}$ are log normally distributed. Taking the log, we obtain the linear law of motion of local infection.

¹⁶We set its mean to be $-\sigma_v^2/2$ so that the expected value of $o_{i,t}$ is unity. This follows from the fact that for a random variable $x \sim N(\mu, \sigma^2)$, the expectation of its exponential $E(\exp(x)) = \exp(\mu + \sigma^2)$

¹⁷For instance, see Eichenbaum et al. (2020) and Krueger et al. (2020).

$$\begin{aligned}
\Xi_{i,t} &= \exp(\psi_t) \exp(\eta_{i,t}) \Xi_{i,t-1} \\
\log(\Xi_{i,t}) &\equiv \xi_{i,t} = \psi_t + \eta_{i,t} + \xi_{i,t-1} \\
\psi_t &= \psi_{t-1} + \theta_t \\
\eta_{i,t} &\sim N\left(-\frac{\sigma_\eta^2}{2}, \sigma_\eta^2\right) \\
\theta_t &\sim N\left(-\frac{\sigma_\theta^2}{2}, \sigma_\theta^2\right)
\end{aligned} \tag{17}$$

Our main assumption is that agents do not have perfect observation of the aggregate transmission ψ_t in real-time. Instead, they form subjective perceptions about it $\tilde{\psi}_{i,t}$ following the learning rule defined in Section 4. In the individual updating, the observed changes in local infections are used as the noisy signals, which consist of the true state ψ_t and noises $\eta_{i,t}$. Under these specific assumptions, the aggregate shock θ_t in this model is a fundamentally relevant and permanent shock for the learning. The local shock is from idiosyncratic changes in infections, which are time-independent noises for belief updating. It instead affects the consumption of individual agents directly.

$$s_{i,t} = \xi_{i,t} - \xi_{i,t-1} = \psi_t + \eta_{i,t} \tag{18}$$

The local infection state $\xi_{i,t}$ affects the time-varying taste shock $\tau_{i,t}$ and individual productivity shock $z_{i,t}$ according to following linear functions.

$$\begin{aligned}
\log(\tau_{i,t}) &= \alpha_s \xi_{i,t} + \tau_{i,t} \\
\log(z_{i,t}) &= \alpha_z \xi_{i,t} + \zeta_{i,t} \\
\tau_{i,t} &\sim N\left(-\frac{\sigma_\tau^2}{2}, \sigma_\tau^2\right) \\
\zeta_{i,t} &\sim N\left(-\frac{\sigma_\zeta^2}{2}, \sigma_\zeta^2\right)
\end{aligned} \tag{19}$$

Logged preference $\tau_{i,t}$ and labor productivity $z_{i,t}$ are both linear functions of the underlying infection state $\xi_{i,t}$ plus i.i.d. shocks $\tau_{i,t}$ and $\zeta_{i,t}$, respectively. Both shocks are normally distributed with standard deviations σ_ζ and σ_τ .¹⁸ α_s and α_z are the loading parameters from the infection to preference and income respectively. Since higher infections are associated with negative income shocks due to layoff, restriction policies and so forth, and a taste shock biases against contact-based consumption, both α_s and α_z are negative by assumption.

5.3 Optimal Consumption

We start by characterizing the optimal consumption policy and sector-specific demand function of the individual consumer. Under perfect understanding of the spreading speed of the virus, individual's optimal consumption depends on local infection $\xi_{i,t}$ together with preference shock $\tau_{i,t}$, wealth in hand $m_{i,t}$ and permanent income $o_{i,t}$. Under learning from friends, the perceived state of infectiousness $\tilde{\psi}_{i,t}$ enters as additional state variable. Individual's value function at time t is therefore evaluated based on her perceived state of the world, $\tilde{\psi}_{i,t}$, the local infection $\xi_{i,t}$, the draw of the taste shock $\tau_{i,t}$ in addition to permanent income $o_{i,t}$ and total wealth $m_{i,t}$.

¹⁸Their means are both adjusted so that the expected value of $\exp(\zeta_{i,t})$ and $\exp(\tau_{i,t})$ are equal to one.

$$V_{i,t}(m_{i,t}, o_{i,t}, \tilde{\psi}_{i,t}, \xi_{i,t}, \tau_{i,t}) = \max_{\{c_{i,c,t}, c_{i,n,t}\}} u(c_{i,t}(c_{i,c,t}, c_{i,n,t})) + \beta \tilde{E}_{i,t} V_{i,t+1}(m_{i,t+1}, o_{i,t+1}, \psi_{t+1}, \xi_{i,t+1}, \tau_{i,t+1}) \quad (20)$$

Notice that the expected value in the above value function is evaluated on the individual-time specific expectation operator, $\tilde{E}_{i,t}()$. Each agent uses her perceived aggregate state $\tilde{\psi}_{i,t}$ at time t to infer the aggregate state ψ_{t+1} in the next period. Following the common practice in many dynamic decision models involving belief updating, we adopt the bounded rationality assumption, i.e. individuals ignore the possibility of future belief updating when evaluating the expected value of their actions. This explains why we write ψ_{t+1} instead of $\tilde{\psi}_{i,t+1}$ within the expectation operator.

Further simplification of the problem can be made since the value function treats the choices in inter-temporal consumption policy and sector-specific demand as one problem. It turns out that we can separately solve the two problems to reduce the number of state variables. This is due to the two-stage budgeting principle. Since the CES aggregator within the period is homothetic, the indirect utility gained within each period from optimal allocation between two sectors becomes independent from the realization of the preference shock. We can first solve the inter-temporal problem by treating the total consumption as the single control variable. The value function associated with the problem can be written as the following.

$$V_{i,t}(m_{i,t}, o_{i,t}, \tilde{\psi}_{i,t}, \xi_{i,t}) = \max_{\{c_{i,t}\}} u(c_{i,t}) + \beta \tilde{E}_{i,t} V_{i,t+1}(m_{i,t+1}, o_{i,t+1}, \psi_{i,t+1}, \xi_{i,t+1}) \quad (21)$$

Applying the Envelope Theorem to the value function, we can obtain the households' Euler

equation associated with the total consumption $c_{i,t}$ as the following.¹⁹

$$\tilde{E}_{i,t}[e^{(1-\rho)v_{i,t+1}}u'_{t+1}(\frac{c_{i,t+1}}{o_{i,t+1}})] = \beta(1+r)u'_t(\frac{c_{i,t}}{o_{i,t}}) \quad (22)$$

Intra-temporal optimality requires proportional allocation between c and n depending on the taste shifter $\tau_{i,t}$. It is solved as an allocation of the total consumption into two categories based on the realized preference and the relative price of the two. We assume the relative nominal price of the two is one.

$$\frac{u_{c_c}(c_{i,c,t}, c_{i,n,t})}{u_{c_n}(c_{i,c,t}, c_{i,n,t})} = \frac{\tau_{i,t}\phi_c}{1-\phi_c} \left(\frac{c_{i,c,t}}{c_{i,n,t}}\right)^{-\frac{1}{\epsilon}} = 1 \quad (23)$$

5.4 Parameter Calibration

The most important two parameters in the model are regarding belief formation λ and k . While direct identification of these two parameters requires individual panel data on beliefs supplemented by their corresponding listening matrix, this is beyond the scope of our paper. Instead, we internally calibrate the two parameters based on the consumption responses to infection shocks. That is, the aggregate consumption response is affected by both k and λ , displayed in Figure ???. We choose the combination of k and λ such that the sensitivity of consumption with respect to contemporaneous local infections is 0.015, as the baseline estimated coefficient from Table 1. At the same time, we know that cross-sectional variations in consumption sensitivity to differently weighted shocks to connected counties reveal the value of λ independently from k .

¹⁹When solving optimal consumption in the presence of permanent income, one commonly used trick is to normalize consumption and asset by the permanent income level to reduce the number of state variables by 1. We do the same following Gourinchas and Parker (2002) and Carroll (2011).

[INSERT FIGURE ?? HERE]

What makes it possible to read off the implied belief parameters conveniently from consumption response is the unintended assumption that the infection shock plays a role of permanent income shock scaled by the income elasticity to infections, α_z . For instance, taking the estimated consumption elasticity with respect to local infection of 0.015 as an example, dividing it by a value of α_z , say 0.1, gives exactly the consumption-implied belief sensitivity of $(1 - \lambda)k = 0.15$.

What is the best estimate of α_z ? Due to limited access to high-frequency cross-sectional income data, we choose not to estimate it externally. We simply choose a baseline value of 0.1, meaning that a 1% percentage increase in local infection leads to a 0.1% drop in income. We see this as a very conservative value regarding the income effect of the COVID19 infections. Note that our model assumes the effects could come from both decentralized decisions such as business shut-downs, layoffs and government restrictions in response to the pandemic.

We set the loading parameter of the infection to the preference α_s to be -0.2 to match an upper-bound value of the estimated elasticity of contact-based spending to local cases of 0.05% reported in the Figure 1. Of course, this needs to be internally consistent with the chosen value of $\alpha_z = -0.1$, which reflects a higher dis-utility of contact-based consumption and guarantees that $\tau_{i,t} < 1$, i.e., infection lowers the weight of the contact sector compared to its steady-state level. Finally, the size of taste shock $\sigma_\tau = 2.9$ is chosen to match the cross-sectional inequality of contact/non-contact-based consumption before the pandemic, as we discuss along Figure 5.

We estimate the parameters of the infection dynamics as described by Equation 17 using the weekly panel of reported cases of U.S. counties between Feb 1st to June 30th. The estimation takes a form of GMM. We first take the double difference of log infections to get the sample analogue of $\theta_t + \eta_{i,t}$. Then a time-fixed effect regression on this residual will decompose the shock into an aggregate and idiosyncratic component. Taking the cross-sample standard-deviation of the time-

fixed effects and the residuals gives the estimates for $\sigma_\theta = 0.1209$ and $\sigma_\eta = 0.209$, respectively.

Besides, one of the novel additions of this model regards the distinction between two sectors of consumption that bear different infection risk. The literature has not provided an estimate regarding the preference parameters associated with the subcategory demand. We therefore rely upon both Consumer Expenditure Survey (CEX) and the card transaction data to infer them. We group reported subcategory consumption series into contact and non-contact-based ones. The steady-state share of contact consumption ϕ_c is then set to be 0.41.

We also estimate the elasticity of substitution (EOS) between the two via a reduced-form regression of the change in one on that of the other. Our estimates suggest an ϵ of 0.75. This indicates that our baseline model assumes the two sectors of consumption are gross complements. We recognize the substantial disagreement on the assumption regarding the substitutability of the two sectors in the recent literature about the pandemic. For instance, Krueger et al. (2020) assumes a baseline EOS of 3 and 11 for the alternative assumptions although no empirical estimates are provided. Guerrieri et al. (2020) discusses the important aggregate demand implications of the value of EOS without taking an empirical stance on it. Given this, we will compare the calibration results by assuming complementarity and substitutability in later sections.

The non-pandemic block of parameters of income process and preferences are standard. The size of permanent income volatility σ_v^2 is set to be $0.01 * 4/11$. The size of transitory income volatility σ_ζ^2 is set to be $0.01 * 4$, both of which are quarterly counterpart of annual volatility commonly used in the literature. This allows us to match the cross-sectional consumption inequality during the run-up of the pandemic (see Figure 5). For our other preference parameters, we follow the standard consumption/saving literature in choosing the preference parameters. Since the model is set at a quarterly frequency, both the time discount factor and interest rates are converted accordingly. In particular, the time discount factor β is $0.99^{1/4}$. The risk-free nominal interest factor $1+r$ is $1.02^{1/4}$.

The relative risk aversion ρ is 2.

The exact procedures of calibration are as followed. (1) Solve the model based on the optimality conditions laid out in the previous section. (2) Simulate the cross-sectional histories of idiosyncratic infections and the corresponding perceptions of individual agents of the aggregate state using the belief updating rule in this paper. (3) Simulate the history of individual consumption streams based on the simulated beliefs and resulting assets and compute the aggregate consumption responses.

6 Counterfactual Experiments

6.1 Benchmark: Pre-pandemic Consumption

Before exploring the implications of the pandemic for the consumption responses, we first calibrate the model for the pre-pandemic period. Specifically, we set the underlying local infection state to be zero $\xi_{i,t} = 0$ deterministically for all agents in the economy. This turns the income process into a standard permanent/transitory two-component process. The relative preference for contact versus non-contact consumption now depends solely on the idiosyncratic and transitory taste shock.

Like many other models featuring with ex-ante homogeneity and uninsured idiosyncratic income risks (Castaneda et al., 2003; Carroll et al., 2017), our model generates ex-post heterogeneity across agents in terms of consumption and wealth. Since the data on cross-county wealth is not available, we focus on consumption inequality. We simulate the pre-pandemic histories of the economy for a long period of time such that the cross-sectional consumption inequality implied from the simulation broadly matches that from the data, giving us a useful benchmark.

Figure 5 plots the simulated and data-implied Lorenz Curves of total and subcategory consumption across all U.S. counties in our data sample before the pandemic. Since we suspect that the

inequality suggested by the raw transaction data is driven by cross-regional differences in the data coverage and other unobservable characteristics, we compute the consumption inequality based on regression residuals of the consumption spending on a broad set of county-specific variables, including: population, GDP per capita, the share of males, the education distribution, and the race distribution. This implies a cross-sectional standard-deviation of log consumption per capita of 0.89 over the period of June 2017 to February 2020. While it is larger than the 0.3 to 0.45 dispersion of log consumption found in other household data, our calibrated parameters nonetheless allow us to broadly match the consumption inequality ([Blundell et al., 2008](#); [Heathcote et al., 2010](#); [Kaplan and Violante, 2010](#); [Heathcote et al., 2014](#); [Aguiar and Bils, 2015](#)).

[INSERT FIGURE 5 HERE]

We can also validate the assumption of the model regarding the two sectors by examining the subcategory consumption inequality. We group detailed card spending data into two sectors as we defined in this paper. Lorenz Curves of contact and non-contact-based consumption, which are shown in the middle and right panel in Figure 5 indicates that the consumption inequality within categories is higher than the total consumption, suggesting the role of heterogeneity in preference shocks. This subcategory inequality helps identify the size of preference shock $\sigma_\tau = 2.9$. We pick this value such that the Lorenz Curves of both categories match that from data, respectively (e.g., [Aguiar and Hurst \(2013\)](#) and [Attanasio and Pistaferri \(2016\)](#)).

Taking the pre-pandemic wealth distribution as the initial condition, we proceed to explore the aggregate consumption responses after the outbreak of the pandemic. At the time $t = 0$, hit a chosen fraction of agents with an infection shock to get the impulse responses of the economy. All impulse responses of the aggregate variables are plotted as the differences relative to the steady-state scenario. It is defined as one where local infections stay at the initial level. It means that

there are no idiosyncratic shocks to local infections, and the aggregate transmission $\psi_t = 0$, namely zero growth in infections. And also assume that all agents start with common and correct prior about the aggregate transmission. At the same time, individuals keep drawing new permanent and transitory income shocks.

6.2 Experiment 1: Different Degrees of Social Communication

We first examine the aggregate responses under imperfect information regarding aggregate transmission with different degrees of social communication (different λ s). $\lambda = 0$ corresponds to the case of zero-social communication. We undertake the analysis fixing the degree of individual responsiveness k at $\kappa^* = 0.33$, the steady-state weight from Kalman filtering computed from estimated volatility of aggregate and local infections (see Appendix A.4 for derivations). This is essentially to assume individuals rationally respond to their local news under imperfect information. Furthermore, the shock is assumed to hit the top one-third nodes according to the influence.

Figure 6 shows the responses of aggregate variables. A 10% increase in infections for a third of the agents corresponds to a 3.3% increase in the average infection in the economy and affects the average wealth via income shock correspondingly. The aggregate belief overreacts compared to the full-information case since by assumption the shocks are not relevant to the fundamental state.

With social communication, the same news will be propagated to the economy along different paths depending on the degree of communication, thus inducing different aggregate consumption responses. A bigger value of λ lowers the initial response to the shock but slows the convergence speed to zero. The L-shaped belief responses under lower social weight induce more consumption spending cut first followed by a faster recovery afterward. In contrast, a moderate hump shape

of belief response under more social communication smooths the responses to noises hence the consumption dynamics. This suggests one of the possible drivers of different recovery patterns might be driven by the interactive effect of individual reactions and social communications.

Quantitatively speaking, moving from zero social communication to a medium level of social communication ($\lambda = 0.5$) implies a smaller drop in spending by 0.1 percentage points in the first period of the shock. The effects on sub-category consumption follows the same token as higher perceived transmission not only lowers total consumption but also induces shifting toward non-contact consumption. Again, this is under the assumption that the income elasticity with respect to local infection is 0.1. A higher value implies a bigger differences in adjustments.

[INSERT FIGURE 6 HERE]

Fixing the degree of social communication at $\lambda = 0.5$, we could explore the consumption responses under different degrees of news responsiveness by individual agents in the model(different k). At the macro level, the effect of higher k and lower λ are similar. Figure 7 plots the responses. Overreaction to the news at the individual level induces a sharp reaction in aggregate belief but more rapid reverse to zero. Lower overreaction in contrast slows the spread of the news in general and smooths both belief reactions and consumption responses.

[INSERT FIGURE 7 HERE]

6.3 Experiment 2: The Location of the Pandemic Shock

Individual nodes have different influences in the network. Therefore, the aggregate responses may differ depending on where the infection shock takes place. Figure 8 plots the impulse response graphs following the same-sized 10% infection increase in the top, middle, and bottom one-third of the nodes in terms of their social influence measured by their degrees. It is not surprising

that aggregate consumption sees the biggest reaction if the infection news takes place in the most influential agents in the economy. Although in all scenarios the initial drop in consumption is equal in size before the social communication, the shocks that hit the top influencers are first amplified via social communications thus inducing a further drop in aggregate consumption before the recovery while the other two scenarios see a gradual recovery following the initial shock. This suggests that the location of the initial shocks may not only affect the overall size of the aggregate demand response, but also its shape of the dynamics.

[INSERT FIGURE 8 HERE]

This location-dependent mechanism of aggregate amplification is very similar in flavor to related macroeconomic work in other contexts such as input-output linkages (Acemoglu et al., 2012; vom Lehn and Winberry, 2020), but the impacts here are belief-driven. As our empirical evidence has shown, a similar mechanism is present with the COVID-19 pandemic: since the infections first hit the metropolitan and well-connected regions such as New York City and Seattle, it is fair to conjecture that this has induced a more sizable drop in aggregate consumption than a counterfactual scenario where the COVID-19 first hit less connected regions.

6.4 Experiment 3: Alternative Network Structure

What would have happened to the consumption responses if the economy is set in a social network of different structures? Figure 10 compares the impulse responses to the same shock based on the social network in 2016, 2019 and an imagined autarky world, respectively. Since Figure A.4 shows that the social influence has grown more dispersed over time, shocks that take place in the most influential nodes will receive greater weight. This gives more room for possible amplification of the local shock via network. Since the network does not affect the initial response, average belief

responses are the same at the time of the shock but play out along different paths.

We set $\lambda = 0.7$ a larger value than our benchmark to show the differences from network more clearly. Individual responsiveness k remains $\kappa^* = 0.33$. As the Figure shows, the belief response in 2016 no longer takes a hump pattern as in 2019 due to the smaller dispersion in influence. An autarky network, not surprisingly, shows a rapid return to zero following the shock due to zero influence from others. Despite the differences in belief patterns, their implied differences in consumption spending end up being negligible in this scenario. All three scenarios witness around a same-sized drop of 0.5% and almost identical consumption recovery following the shock.

Of course, for higher sensitivity of income to the infection or more overreaction to the news at the individual level, the differences in the macroeconomic impacts by different networks will be more significant. We take this evidence as assuring regarding our modeling assumption that the weight matrix is time-invariant. Our conjecture is that the slow-moving nature of the social networks at the macro level will not fundamentally change the macroeconomic responses. The results help confirm this. However, we remain cautious about overinterpreting these results because the alternative network structure could have much higher dispersion in influences than the observable ones. It is nonetheless clear that a more asymmetric network will increase the chance that any local shocks, especially those that hit the influential does, contribute to aggregate effects.

[INSERT FIGURE 10 HERE]

6.5 Experiment 4: Substitution and Complementarity

In the results thus far, we maintain the assumption that the two sectors of consumption are gross complements. We now compare the impulse responses of following the same shock under a range of values of EOS, 0.75, 0.99 and 1.5. The first is the baseline value we use in the paper. The second

represents a case close to unit elasticity. The third is when the two sectors become substitutes. Not surprisingly, although the aggregate consumption responses remain the same, the sub-category consumption responses vary substantially depending on the two sectors being substitutable or complementary in consumer's preferences.

Figure 9 presents the scenario with more substitution the 0.5% drop in total consumption consists of 1.0% in contact consumption and a 0.2% drop in non-contact consumption. In contrast, the scenario with complementarity implies a different reallocation: 0.8% drop in contact consumption and 0.4% drop in non-contact based consumption.

[INSERT FIGURE 9 HERE]

Such heterogeneity in sectoral reallocation has important implications for the macroeconomic effects of the pandemic. First, through the general equilibrium effect, a higher degree of substitution will help mitigate the drop in aggregate consumption. Second, if we further allow the consumption behaviors to endogenously affect the infection, higher substitutability across sectors also reduces the infection risk exposure as a whole. Although our model does not incorporate both mechanisms, these effects are rather self-explanatory.

6.6 Discussion

Although our model built in this paper is tailored towards understanding the quantitative effects of the pandemic on consumption, the framework is flexible and it carries broader implications for how social networks can have an aggregate effect in a more general macroeconomic setting. The core structure of the framework is that individual agents form beliefs about some unobservable aggregate state of the economy via private updating of noisy local signals and social communication. We show in such an environment, the impacts of a higher degree of social communication also

depend on individual responses to their own news. Higher social influence moderate beliefs swing by counterbalancing overreactions to noises. But this comes at the cost of slower learning at the society level. By this token, the welfare effects from higher social communication crucially depend on the nature of the shocks as well as the degree of irrationality of individuals.

The presence of interpersonal influences on beliefs hence resulting interconnection in behaviors poses an important question on how to think about the impacts of local/idiosyncratic shocks at the aggregate level. Due to asymmetric influences of different agents in the network, even independently drawn shocks across the economy induces non-balanced responses to the news at the aggregate level. The effect tends to be higher with more overreaction by individuals. Our paper suggests that acknowledging these effects is important when considering the macroeconomic effects of local shocks. This point is essentially very similar to the rapidly developing literature on the production networks and their macroeconomic effects ([Acemoglu et al., 2012](#); [Baqae and Farhi, 2018](#)), although our focus is on interpersonal influences via beliefs.

What this paper does not fully explore are the implications of social communication on belief heterogeneity and how it interacts with market incompleteness. On one hand, social learning induces more convergence in beliefs among individuals due to mutual influence, on the other hand, the slow-spreading nature in such an environment also leads to non-monotonic patterns of cross-sectional belief dispersion. Combined with ex-post heterogeneity in wealth and the marginal propensity to consume from uninsured income shocks, the cross-sectional consumption responses as well as its inequality properties will be different. We leave this for future work to explore.

7 Conclusion

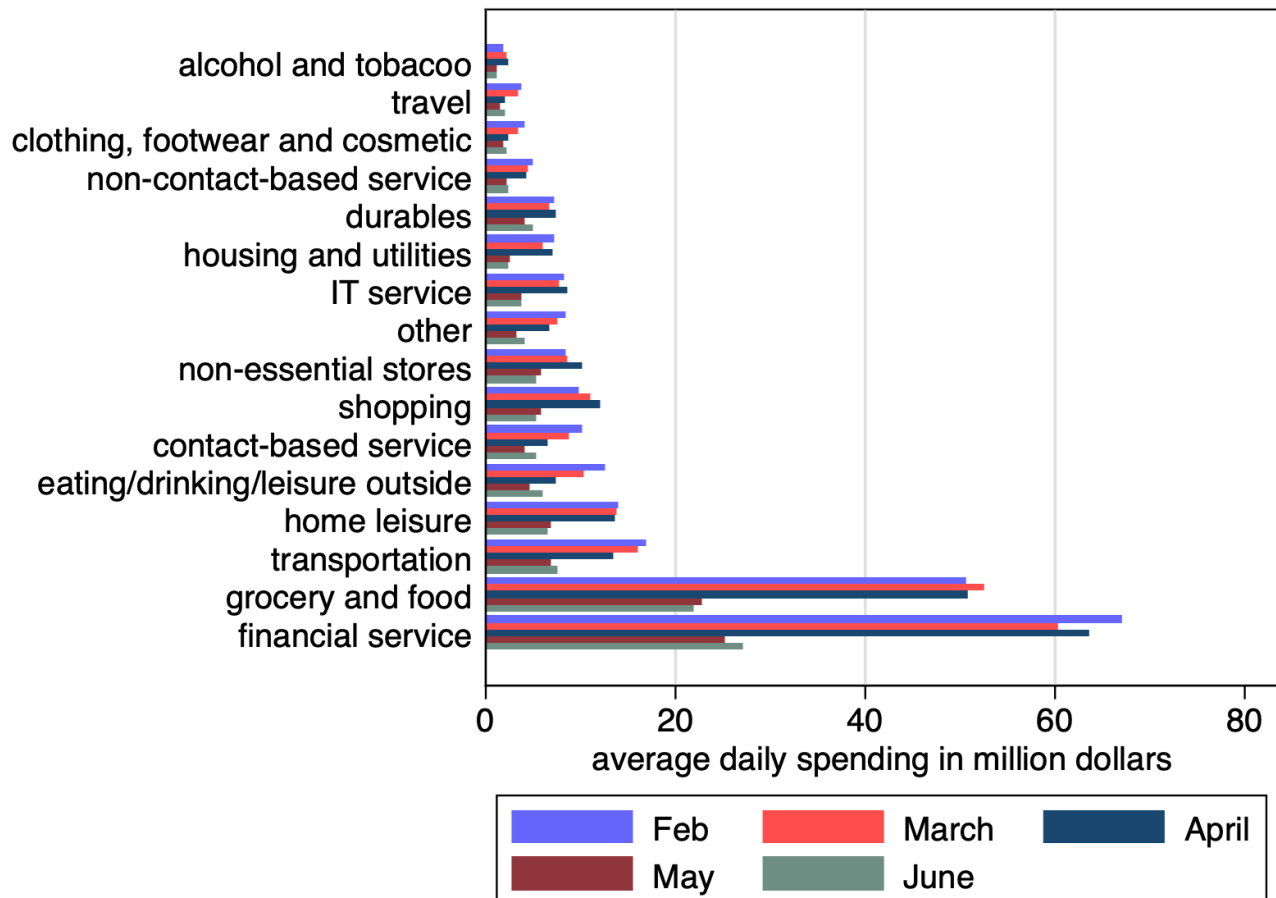
How are economic behaviors such as consumption affected by social communication and information disseminated via online networks? What are their implications for macroeconomic shock propagation mechanisms? This paper tackles these questions both empirically and theoretically.

We first identify the effects of using 5.18 million debit card users' transactions across the United States during COVID-19 and large-scale online social networks. We found significant consumption adjustments in responses to the infection news in one's socially connected counties/foreign countries.

We also construct a heterogeneous agent model featuring belief updating from both private signals and social communications. We show how social communication may moderate overreaction to irrelevant local news in the aggregation but also slows down the belief adjustment to fundamentally relevant shocks. The model also shows how shocks to different locations of the social network can amplify and propagate macroeconomic fluctuations, especially for consumption. Future research should incorporate microeconomic data directly on beliefs linked with consumption and the social network so that the parameters governing the belief formation process can be more precisely identified and more sophisticated theories of belief formation can be tested.

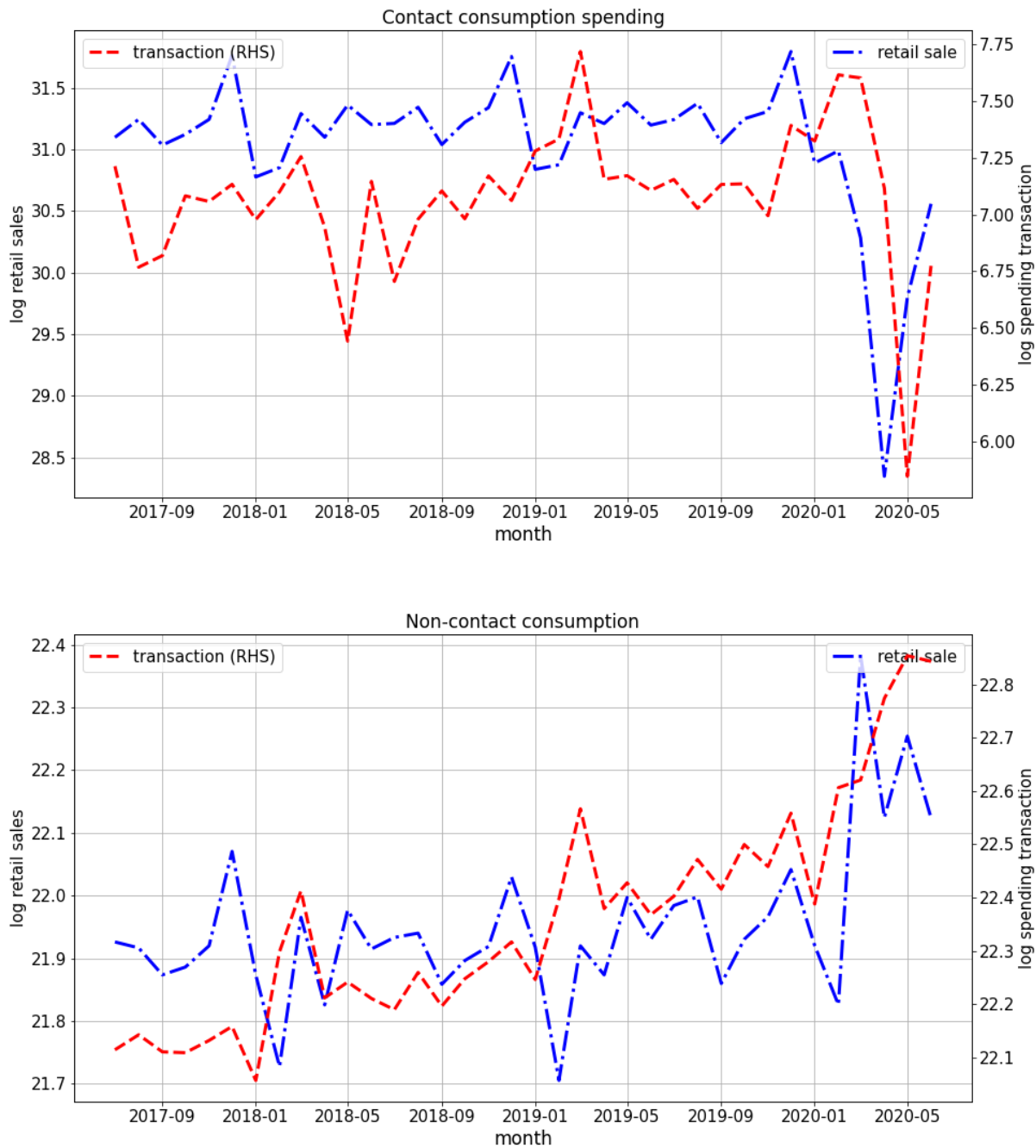
Tables and Figures

Figure 1: Descriptive Statistics on Consumption Expenditures, by Category



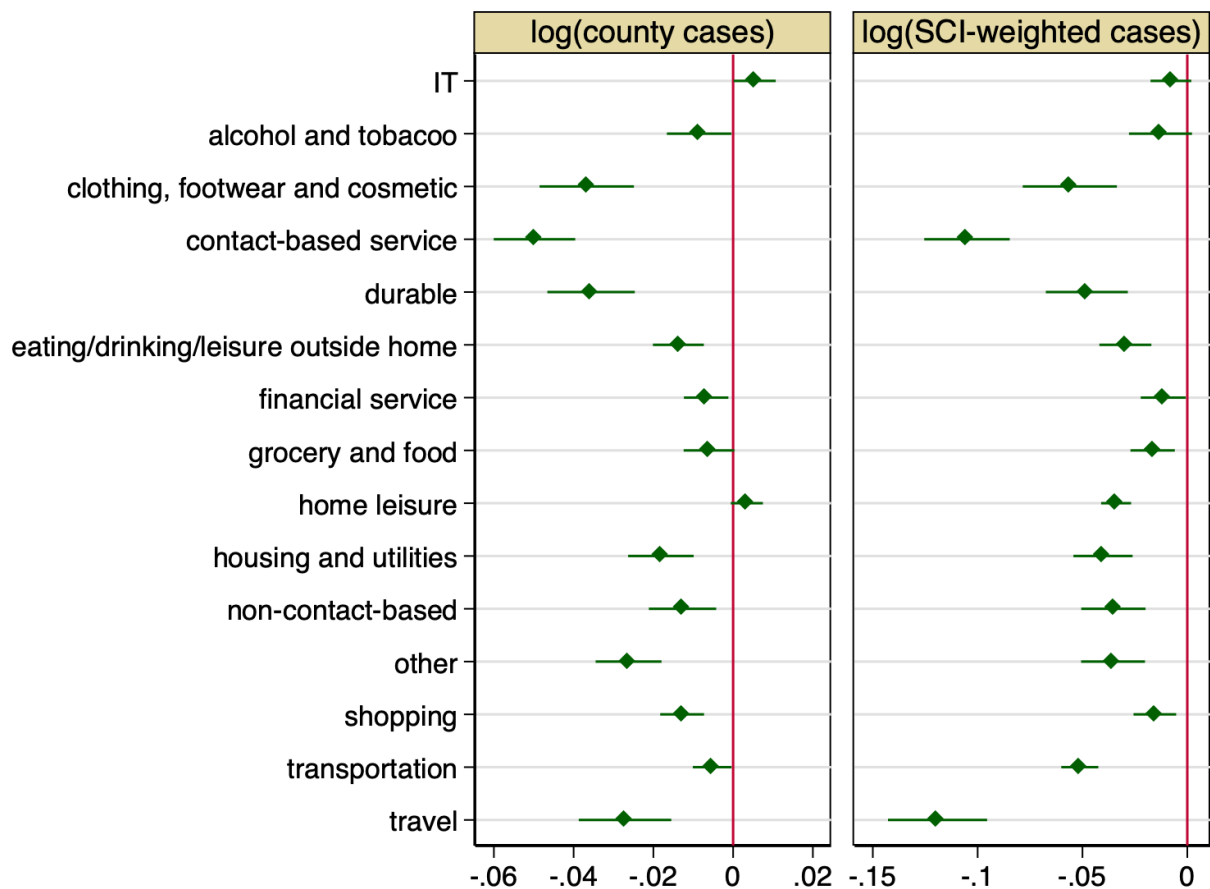
Notes.—Source: Facteus. Average daily consumption by category. Each bar plots the average spending per day in the specific category within each month. See the Appendix for the examples of each consumption category.

Figure 2: Benchmarking Consumption Expenditures with Retail Sales Over Time



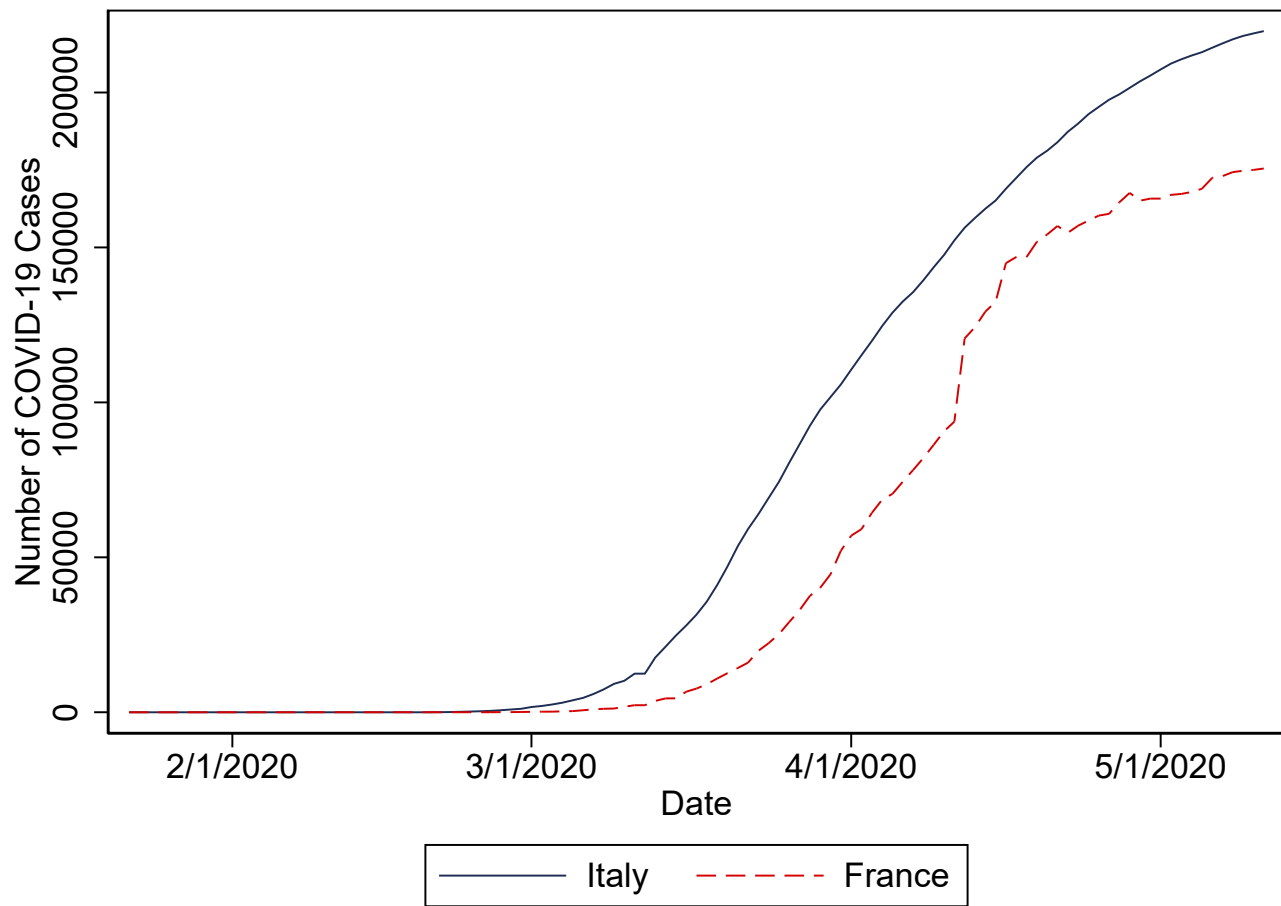
Notes.—Source: retail sales from the Census Bureau and transaction data from Facteus from June 2017 to June 2020. The upper and bottom figures plot the contact and non-contact consumption, respectively. See the appendix for the classification of card transactions. Both retail sales and transactions are without seasonal adjustment and deflated by the PCE price index. Contact-based consumption for retail sales is approximated by the sum of “drinking and eating place” (RSFSDP) and “health and personal care” (RSHPCS). The non-contact consumption is approximated as the total of “grocery stores” (RSGCS) and “food and beverage stores” (RSDBS). The correlation coefficient of the two series is 0.26 and 0.55 on the top and bottom, respectively.

Figure 3: Consumption Response to COVID-19 Shocks, by Consumption Category



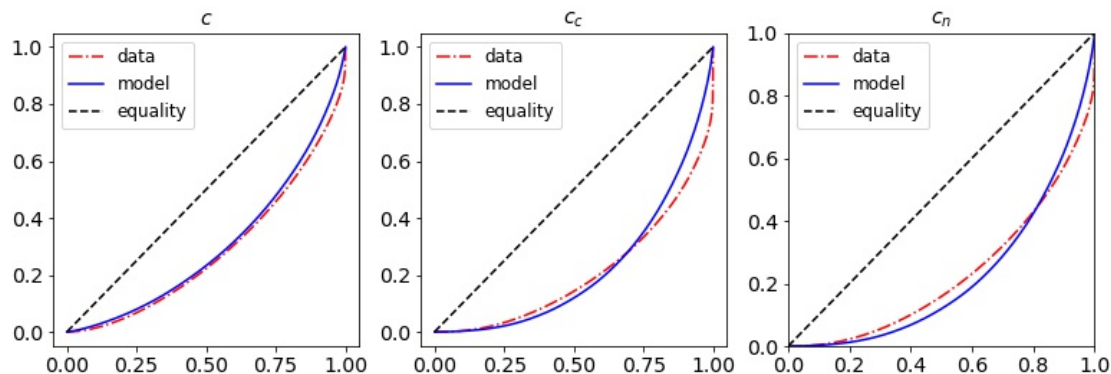
Notes.—Source: Facebook 2019 Social Connectedness Index (SCI) and Facteus. The figure reports the coefficients associated with regressions of logged consumption in a county on the logged number of COVID-19 cases (Panel A) and the logged number of SCI-weighted cases (Panel B) by category of consumption. Each transaction is classified as one of the following category based on its merchant category code (MCC). The sample period is between March 1st to June 30th, 2020

Figure 4: Time Series Patterns in COVID-19 Infections: Italy and France



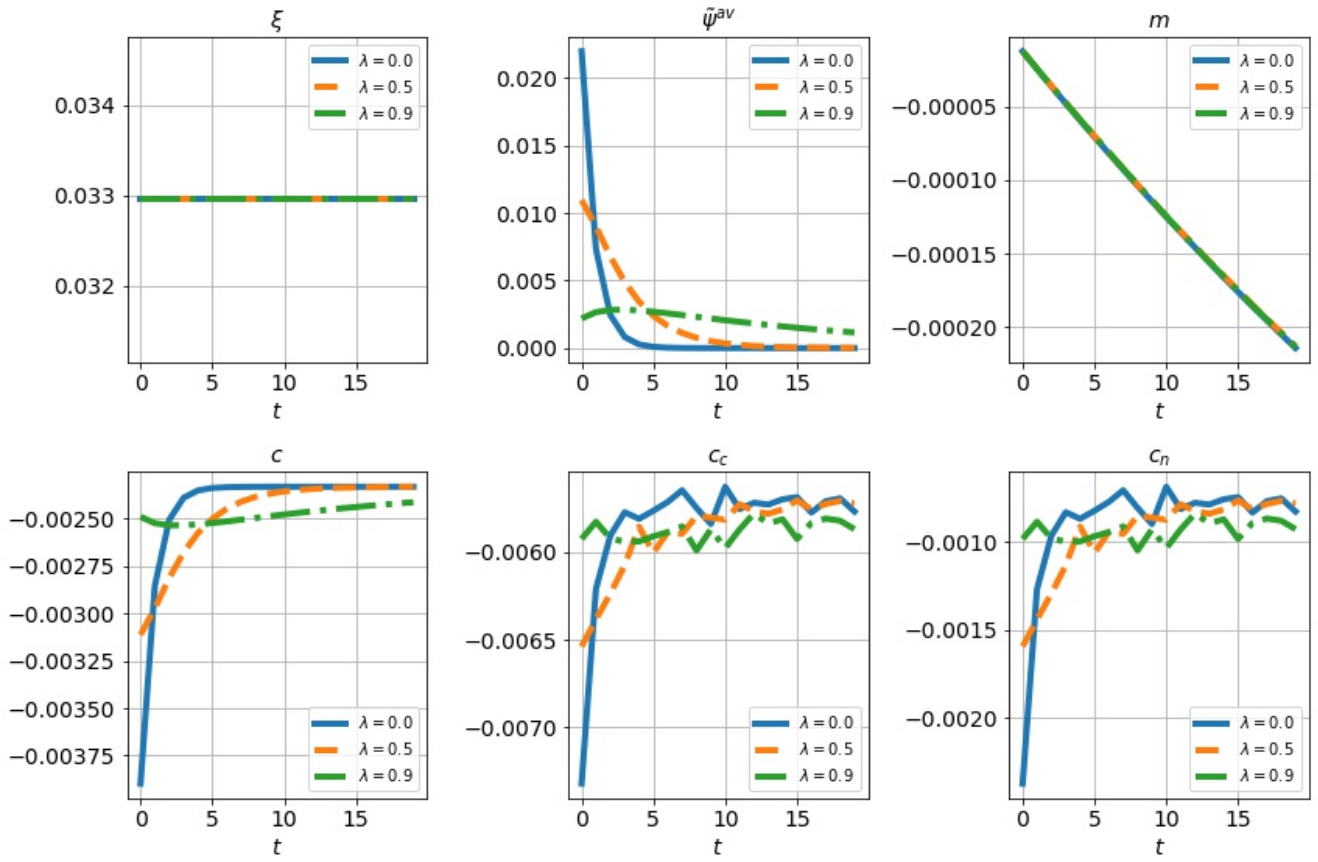
Notes.—Source: Johns Hopkins. The figure plots the number of COVID-19 infections for Italy and France over time.

Figure 5: Lorenz Curve of Cross-county Consumption Before the Pandemic



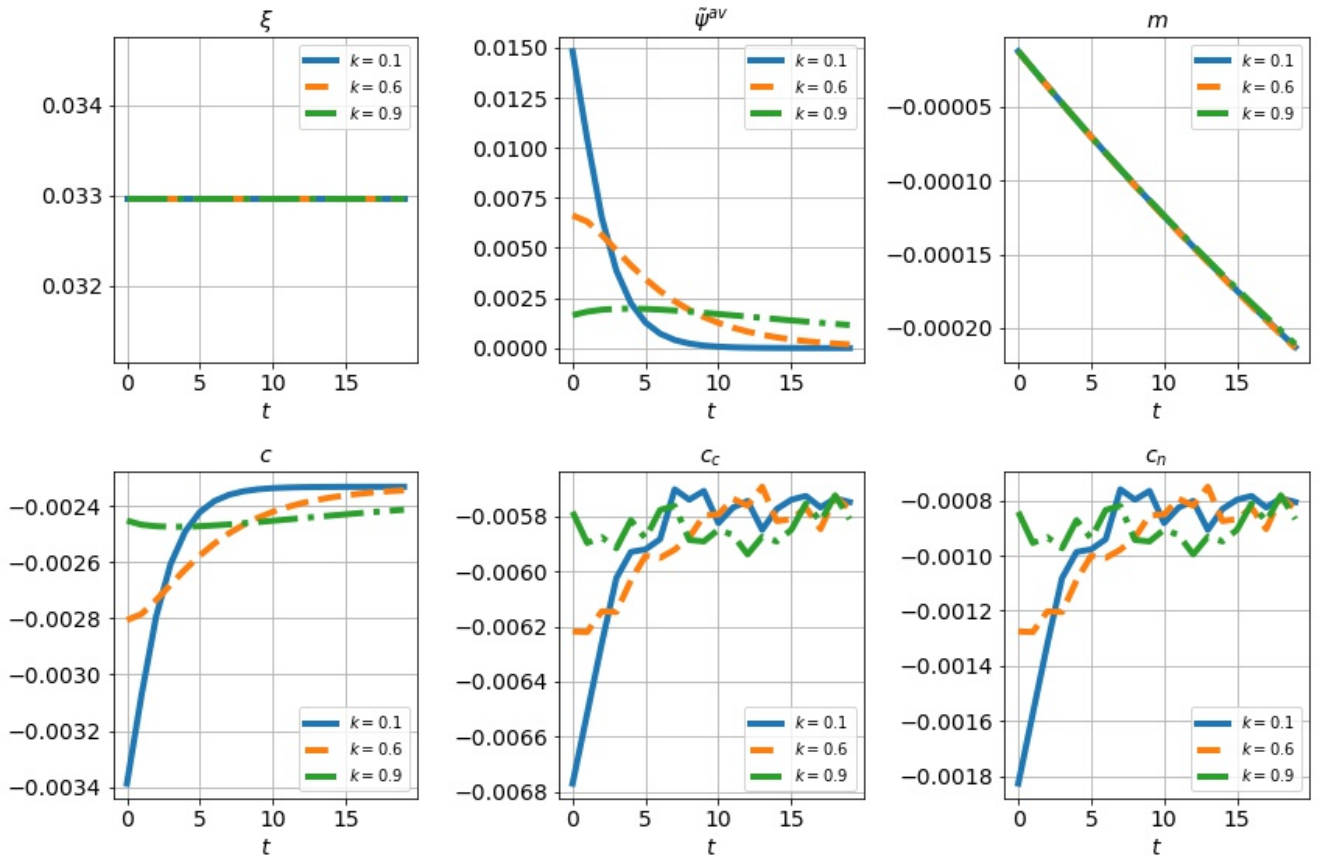
Note: This plot compares the Lorenz Curves of consumption across counties computed from data and simulated from the model. Consumption from data is based on the regression residuals of county-level spending on a list of county-specific demographics. Average consumption between January and February 2020 is used.

Figure 6: Impulse Responses of the Economy to An Infection Shock at Different Degrees of Social Communication



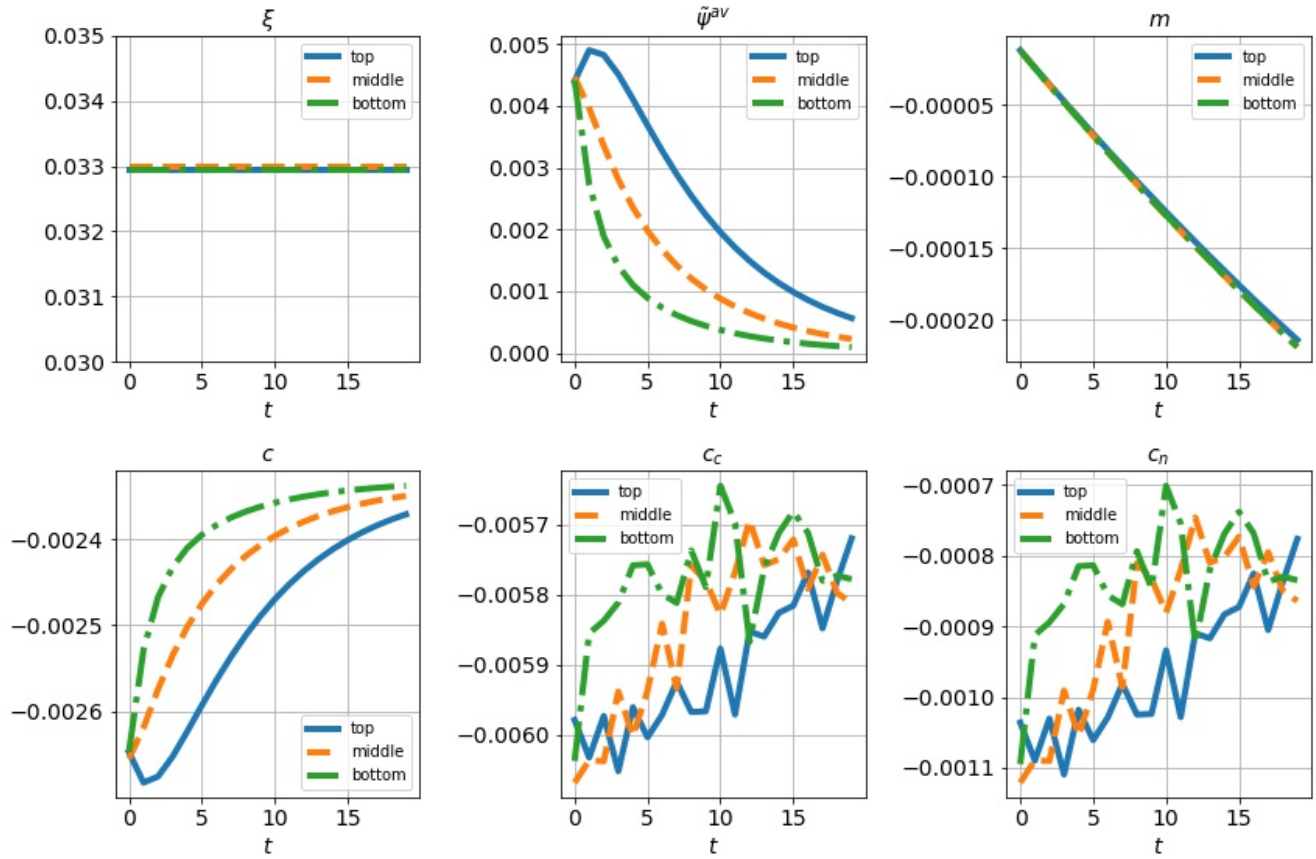
Note: This figure compares the impulse responses of the economy with and without social network influence following a 10% increase in one third of the agents in the economy whose average degree is greater than 1 at time $t = 0$. The variables are average local infection ξ , average perceived transmission $\tilde{\psi}^{av}$, average wealth m , average total consumption c and average contact-based consumption c_c , and average non-contact consumption c_n .

Figure 7: Impulse Responses of the Economy to An Infection Shock at Different Degrees of Individual Responsiveness to News



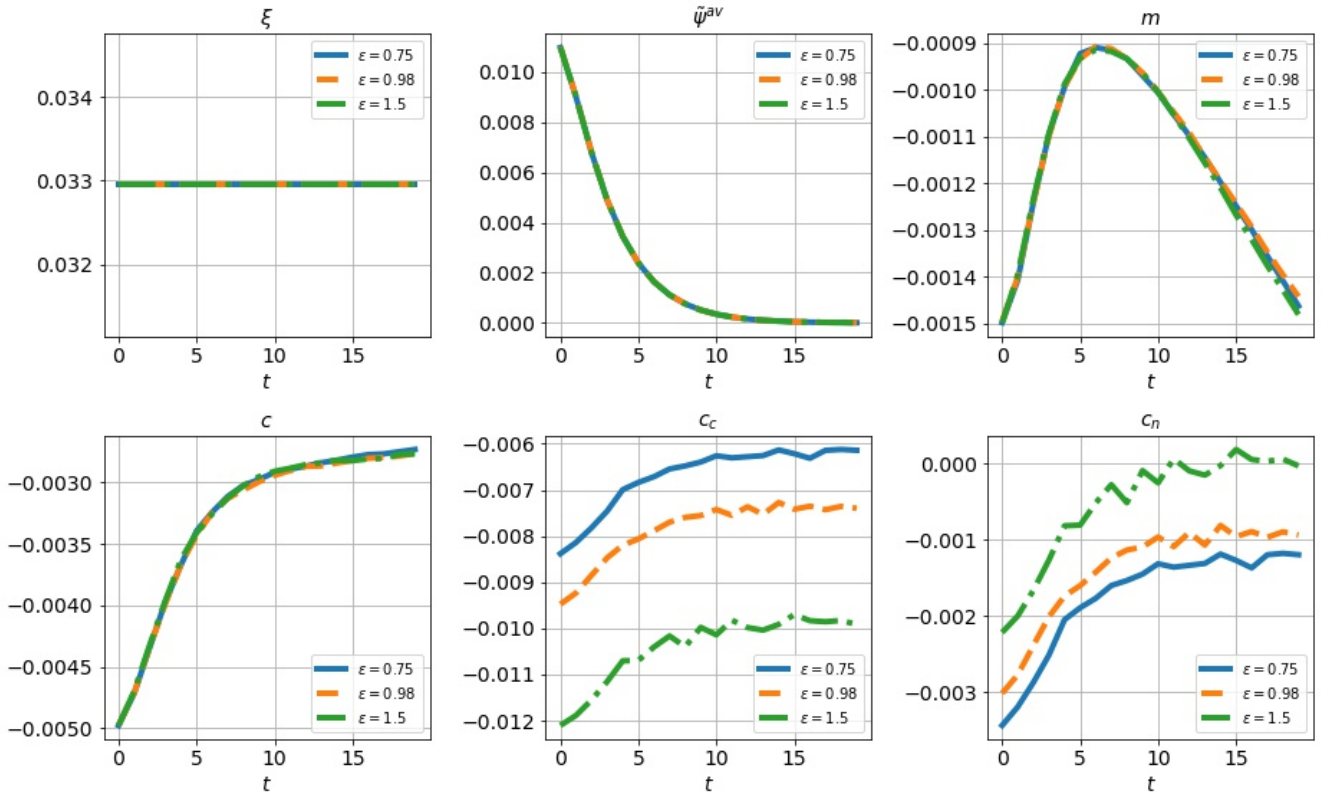
Note: This figure compares the impulse responses of the economy with and without social network influence following a 10% increase in one third of the agents in the economy whose average degree is greater than 1 at time $t = 0$. The variables are average local infection ξ , average perceived transmission $\tilde{\psi}^{av}$, average wealth m , average total consumption c and average contact-based consumption c_c , and average non-contact consumption c_n .

Figure 8: Impulse Responses of the Economy to An Infection Shock in Nodes of Different Influences



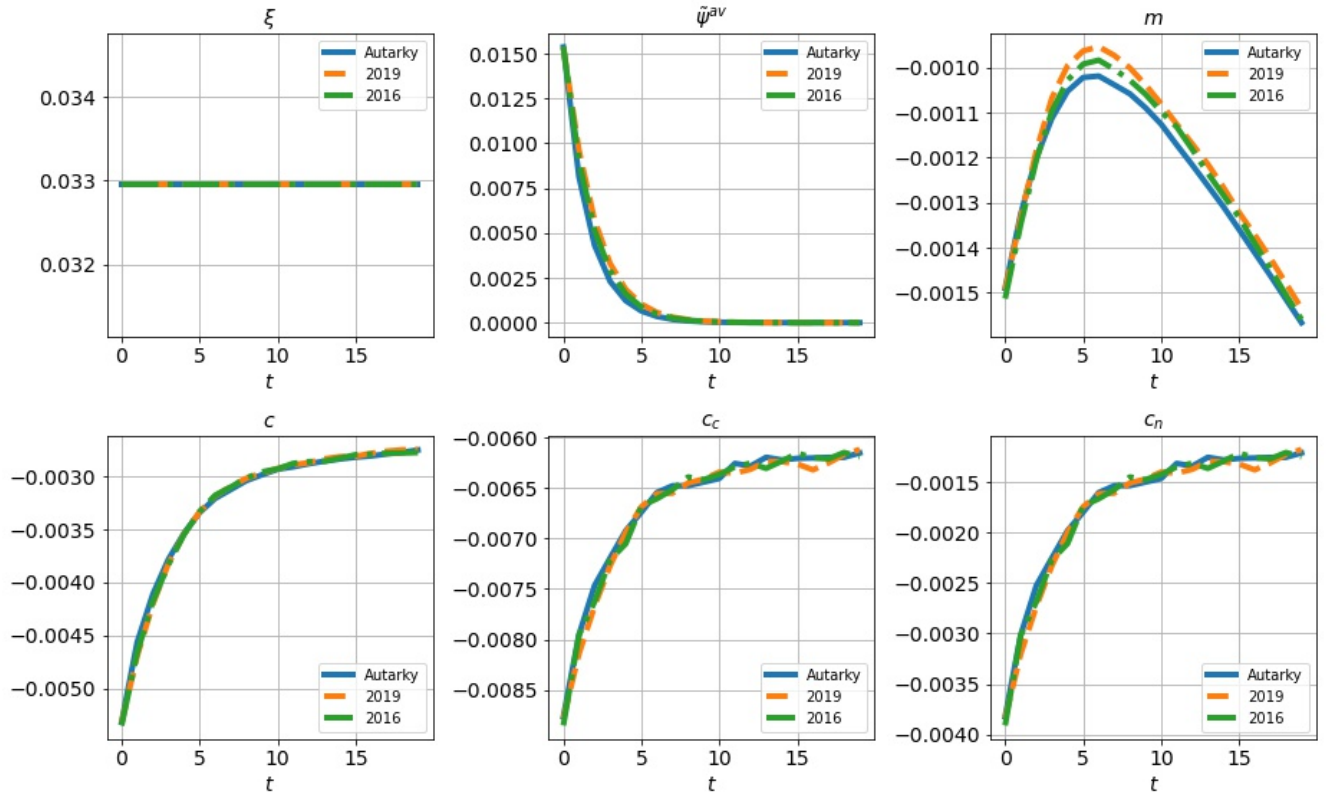
Note: This figure compares the impulse responses of the economy following a 10% increase in a random top/middle/bottom third fraction of the most influential agents in the economy at time $t = 0$. The variables are average local infection ξ , average perceived transmission $\tilde{\psi}^{av}$, average wealth m , average total consumption c and average contact-based consumption c_c , and average non-contact consumption c_n .

Figure 9: Impulse Responses of the Economy to An Infection Shock: Different EOS between Contact and Non-contact Consumption



Note: This figure compares the impulse responses of the economy following a 10% increase in the top one third most influential nodes in the economy at time $t = 0$ under degree of elasticity of substitution between two sectors. The variables are average local infection ξ , average perceived transmission $\tilde{\psi}^{av}$, average wealth m , average total consumption c and average contact-based consumption c_c , and average non-contact consumption c_n

Figure 10: Impulse Responses of the Economy to An Infection Shock: Social Network at Different Times



Note: This figure compares the impulse responses of the economy following a 10% increase in the top one third most influential nodes in the economy at time $t = 0$ under the social network in 2016 and 2019. The variables are average local infection ξ , average perceived local infection $\tilde{\xi}$, average wealth m , average total consumption c and average contact-based consumption c_c , and average non-contact consumption c_n .

Table 1: Consumption Responses to Increases in Socially-connected Coronavirus Cases and Deaths

Dep. var. =	log(Consumption Expenditures)									
	(1)	(2)	(3)	(4)	(5)	(6)	(7)	(8)	(9)	(10)
Has SAHO			-.058*** [.005]	.007 [.012]	-.058*** [.005]			-.056*** [.005]	-.044*** [.005]	-.060*** [.005]
log(SCI-weighted Cases)	-.051*** [.007]	-.015* [.008]	-.014* [.008]	-.003 [.009]						
× SAHO				-.024*** [.004]						
log(SCI-weighted Deaths)							-.062*** [.008]	-.042*** [.010]	-.063*** [.012]	-.049*** [.013]
× SAHO									-.026*** [.005]	
log(SCI-weighted Cases, Other States)							-.016* [.009]			-.059*** [.012]
log(SCI-weighted Deaths, Other States)										-.003 -.005
log(County Cases)	-.015*** [.004]	-.006* [.004]		-.006 [.004]	-.006* [.004]			-.013*** [.004]	-.003 [.003]	
log(County Deaths)	-.015*** [.004]	-.018*** [.003]	-.018*** [.003]	-.017*** [.003]	-.017*** [.003]			-.006* [.004]	-.008** [.004]	-.007* [.004]
R-squared	.97	.97	.97	.97	.97	.97	.97	.97	.97	.97
Sample Size	351645	351645	351645	351645	351645	351645	351645	351645	351645	351645
County FE	Yes	Yes	Yes	Yes	Yes	Yes	Yes	Yes	Yes	Yes
Time FE	Yes	Yes	Yes	Yes	Yes	Yes	Yes	Yes	Yes	Yes
State Policies	No	No	Yes	Yes	Yes	No	No	Yes	Yes	Yes
State × Month FE	No	No	Yes	Yes	Yes	No	No	Yes	Yes	Yes

Notes.—Sources: Facebook Social Connectedness Index (SCI) for 2019, Facteus. The table reports the coefficients associated with regressions of logged consumption spending on logged SCI-weighted infections (excluding county c 's friendship ties with itself) and logged county infections and deaths, conditional on county and time fixed effects. Consumption is deflated by the national personal consumption expenditure index. Our SCI-weighted cases and death index is constructed as follows: $COVID_{c,t}^{SCI} = \sum_{c'} (COVID_{c',t} \times SCI_{c,c'})$ where $COVID_{c',t}$ denotes the logged SCI-weighted number of cases or deaths in county c' , and $SCI_{c,c'}$ denotes our measure of the SCI. We normalize the scaled number of friendship ties in a county to its total number of friendship ties, thereby exploiting the relative exposure to other locations. Our variables that are denoted “other states” construct the SCI excluding counties within the same state to control for physical proximity. Standard errors are clustered at the county-level. The sample period is between March 1st to June 30th, 2020.

Table 2: Heterogeneous Effects of the COVID-19 Information Shock on Consumption, by County Characteristics

RHS Variable Partition =	Per Capita Income		Share Under Age 35		Share Over Age 65		Population		Digital Intensity		Teleworking Intensity		
	High	Low	High	Low	.014	-.028***	.007	-.040***	.007	-.038***	.009	-.042***	-.031***
log(SCI-weighted Cases)	-.012 [.010]	-.047*** [.014]	-.021** [.010]	-.025** [.011]	-.014 [.012]	-.028*** [.010]	-.044*** [.008]	-.044*** [.015]	-.040*** [.009]	-.038*** [.012]	-.042*** [.009]	-.042*** [.012]	-.031*** [.011]
log(County Cases)	-.009 [.006]	-.004 [.005]	-.002 [.005]	-.010 [.007]	-.004 [.007]	-.008 [.005]	-.013*** [.005]	-.008 [.005]	-.014* [.007]	-.020*** [.007]	-.013* [.008]	-.020*** [.008]	-.020*** [.006]
log(County Deaths)	-.021*** [.005]	-.008 [.004]	-.006 [.006]	-.017** [.007]	-.008 [.004]	-.017** [.004]	-.001 [.004]	.008** [.004]	-.039*** [.010]	.019*** [.007]	.011* [.007]	.015** [.007]	.014** [.006]
R-squared	.97	.96	.97	.95	.94	.98	.98	.89	.98	.98	.97	.97	.98
Sample Size	168408	169458	170209	167657	165469	172397	180275	157591	26823	24096	25876	25043	
County FE	Yes	Yes	Yes	Yes	Yes	Yes	Yes	Yes	Yes	Yes	Yes	Yes	
Time FE	Yes	Yes	Yes	Yes	Yes	Yes	Yes	Yes	Yes	Yes	Yes	Yes	

Notes.—Sources: American Community Survey (2014-2018), Facebook Social Connectedness Index (SCI) for 2019, Facteus. The table reports the coefficients associated with regressions of logged consumption spending on logged SCI-weighted infections (excluding county c 's friendship ties with itself) and logged county infections and deaths, conditional on county, time, and state \times month fixed effects, separately for different groups that partition the county (or in the case of digital and telework intensity, the state) based on whether the value ranks above the median of the distribution. Digital and teleworking intensities are obtained from Cellipoli and Makridis (2018) and Dingel and Neiman (2020). Consumption is deflated by the national personal consumption expenditure index. Our SCI-weighted cases and death index is constructed as follows: $COVID_{SCT}^{SCI} = \sum_{c'} (COVID_{c',t} \times SCI_{c',t})$ where $COVID_{c',t}$ denotes the logged SCI-weighted number of cases or deaths in connected counties, $COVID_{c',t}$ denotes the logged number of cases or deaths in county c' , and $SCI_{c',t}$ denotes our measure of the SCI. We normalize the scaled number of friendship ties in a county to its total number of friendship ties, thereby exploiting the relative exposure to other locations. Standard errors are clustered at the county-level. The sample period is between March 1st to June 30th, 2020.

Table 3: Consumption Responses to COVID-19 Information from Other Countries

Dep. var. =	log(spending)				SK			
	ITA	ITA	SPA	FRA	ITA	SPA	FRA	SK
log(SCI-weighted cases of the country)	-.007*** [.001]		-.008*** [.001]			-.011*** [.001]		-.011*** [.001]
log(SCI-weighted deaths of the country)		-.052*** [.001]			-.072*** [.001]		-.014*** [.001]	-.081*** [.002]
log(County Cases)	-.005 [.003]	.015*** [.004]	-.005 [.003]		.003 [.004]	-.005 [.003]	-.005 [.003]	.012*** [.002]
log(County Deaths)	-.004 [.016]	-.025 [.018]	-.004 [.016]		-.019 [.018]	-.004 [.016]	-.004 [.016]	-.005 [.003]
R-squared	.97	.98	.97		.98	.97	.97	.98
Sample Size	78550	62925	78550		34148	78550	78550	65552
County FE	Yes	Yes	Yes		Yes	Yes	Yes	Yes
Day FE	No	No	No		No	No	No	No

Notes.—Sources: Facebook, Factens. The table reports the coefficients associated with regressions of logged consumption spending on logged SCI-weighted infections or deaths of a given foreign country, conditional on county and time fixed effects. These SCI-weighted infections / deaths are obtained by taking the time-varying number of infections in country i and multiplying it by the exposure of county c to country i , producing a Bartik-like measure. The four countries are Italy(ITA), Spain (SPA), France (FRA) and South Korea (SK). The sample period is between February 15th and March 15th, 2020. Standard errors are clustered at the county-level.

A Online Appendix

A.1 Data Description: Consumption Classification

Grocery and food. 1. grocery stores and super markets; 2. convenience stores; 3. drug stores and pharmacies; 4. miscellaneous retail stores; 5. meat provisions; 6. bakery, etc.

Transportation. 1. bus lines; 2. railway stations 3. car rentals; 4. toll and bridge fees, etc.

Home leisure. 1. TV cable fees; 2. digital goods, i.e. games, etc.

Housing and utilities. 1. housing rent payment; 2. home utilities, etc.

Shopping. 1. department stores; 2. discount stores; 3. variety stores; 4. general merchandise; 5. wholesale clubs, etc.

Eating, drinking, and leisure outside the home. 1. restaurants; 2. bars/taverns/clubs; 3. different kinds of parks; 4. outdoor sport and sports events; 5. orchestra and theaters, etc.

Information technology services. 1. computer network; 2. telegraph; 3. telecommunication, etc.

Contact-based services. 1. barber and beauty shops; 2. child care; 3. home cleaning; 4. repair stores; 5. veterinary services; 6. home furnishing; 7. laundry; 8. auto repair, etc.

Durables. 1. vehicles/motorcycle /auto parts; 2. furniture; 3. home appliances; 4. electronics and equipment; 5. home supplies; 6. music instruments, etc.

Non-contact-based services. 1. accounting/auditing; 2. business services; 3. programming; 4. consultations; 5. horticultural/ landscaping, etc.

Clothing, footware, and cosmetics. 1. clothing stores of different kinds; 2. cosmetic stores; 3. footwear and shoe stores, etc.

Alcohol and tobacco. 1. package stores selling wine, beer and other liquor; 2. cigar and tobacco

stores, etc.

Travel. 1. airlines; 2. lodging and hotels; 3. duty-free stores; 4. airports; 5. travel agencies, etc.

Financial services. 1. insurance; 2. money orders; 3. wire transfers, etc.

Other. 1. public organizations; 2. government fees; 3. educations; 4. medical spending such as a dental clinic, etc.

In our model with two broad sectors of consumption, contact-based consumption includes transportation, shopping, eating/drinking/leisure outside the home, contact-based services, durables, clothing/footwear, and cosmetics travel. Non-contact consumption includes grocery and food, home leisure, housing and utilities, information technology services, non-contact-based services, alcohol and tobacco, and financial services.

A.2 Data Description: Social Connectedness Index

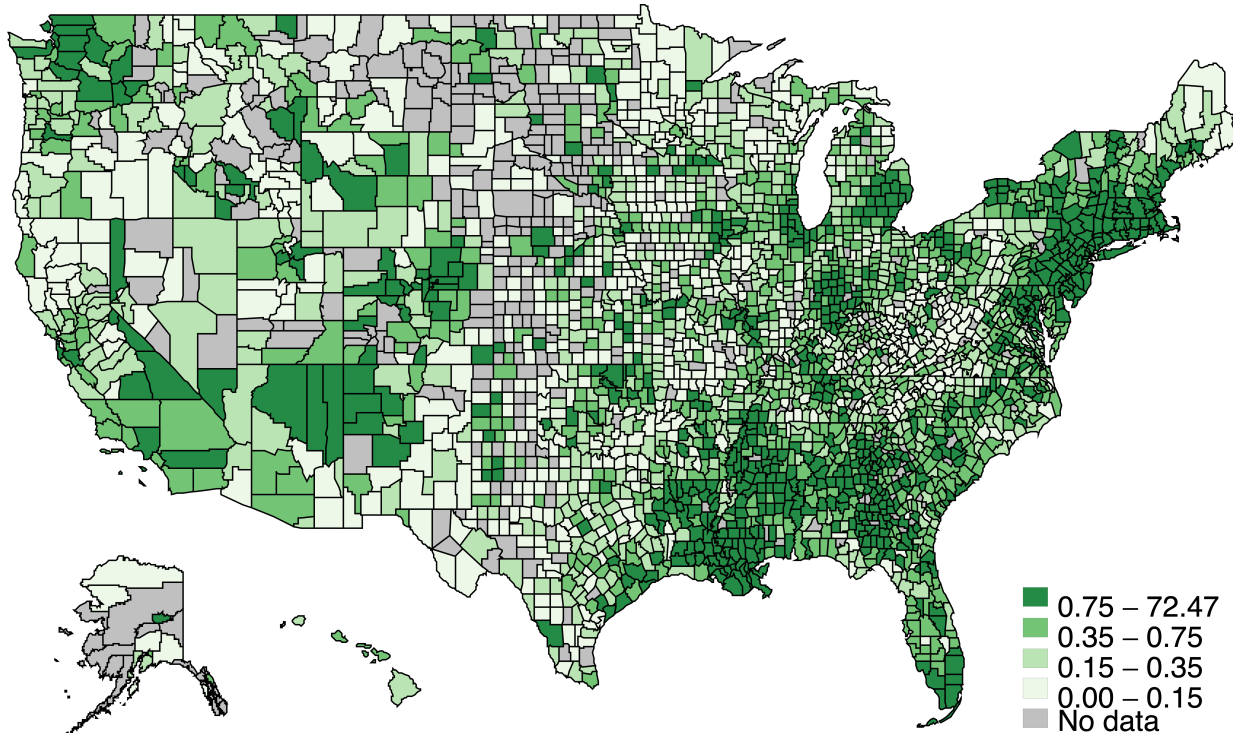
Figures A.1 and A.2 characterize the spatial distribution of not only infections and deaths, but also SCI-weighted cases and deaths based on exposure to connected counties as of April 1, 2020. While the actual number of infections or deaths in county c are correlated with their SCI-weighted versions, they display important differences. In particular, the correlation is only 0.40 between infections / deaths and their SCI counterparts. Moreover, the correlation is roughly half as large when comparing SCI-weighted infections and deaths or infections and SCI-weighted deaths.

Figure A.3 presents the heat map corresponding to the listening matrix using 2019 SCI data. It demonstrates the significant variability across counties.

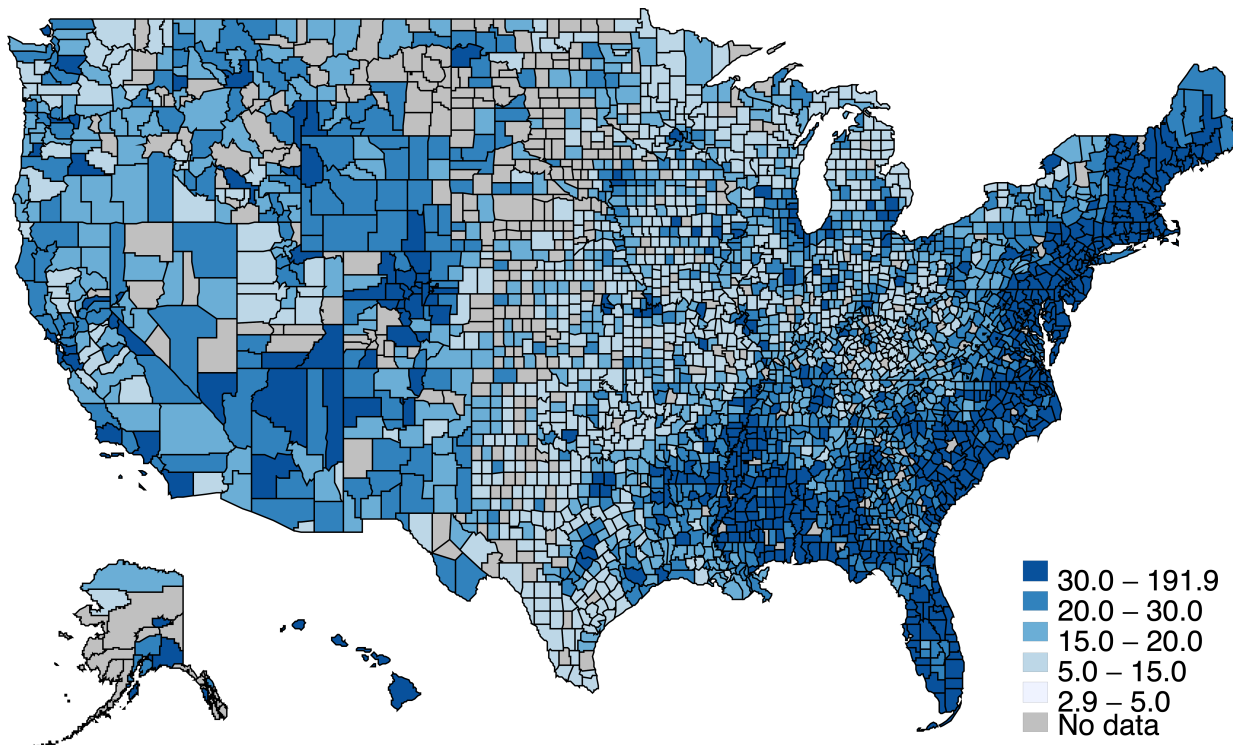
Figure A.4 plots the distribution of degrees from the SCI in the years 2016 and 2019, respectively. The distribution is right-skewed with a long tail. This indicates a small fraction of nodes has a disproportionately strong influence within the network. By construction, the average degree in the

Figure A.1: Actual and Socially-connected COVID-19 Case Infections

Nb of cases per thousand (Apr 1st 2020)



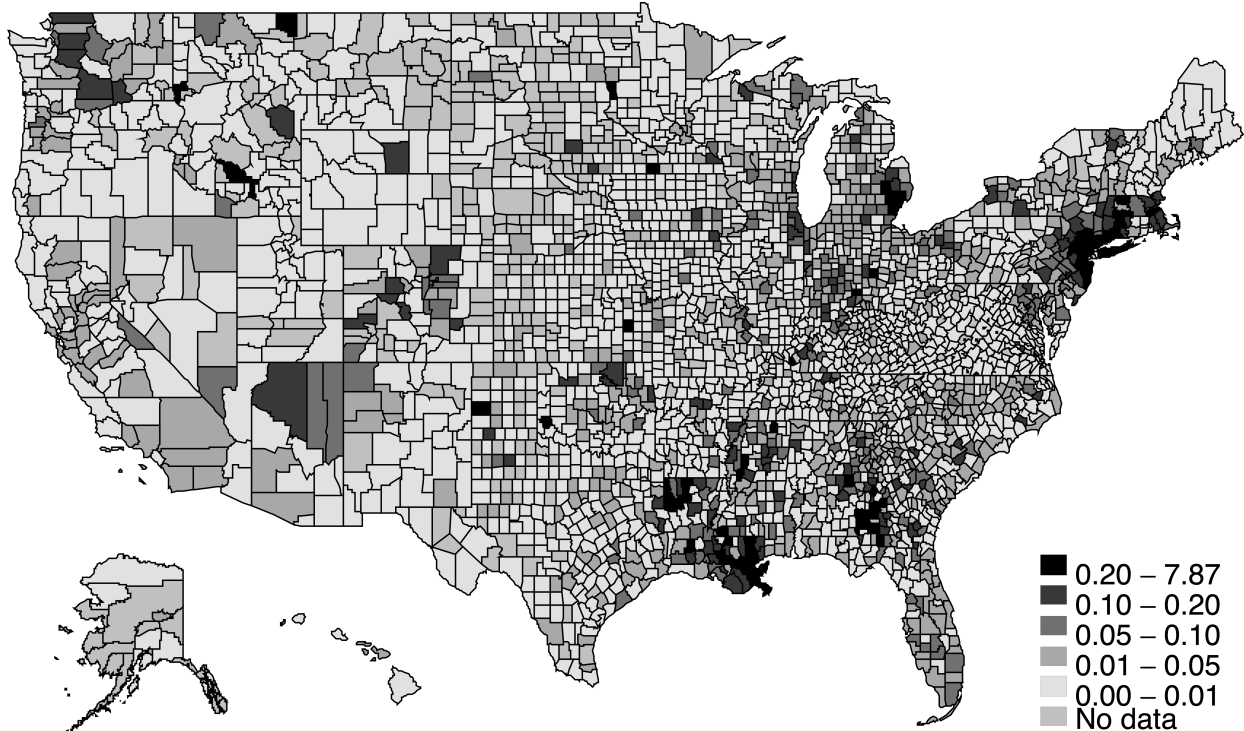
Nb of cases per thousand on Facebook (Apr 1st 2020)



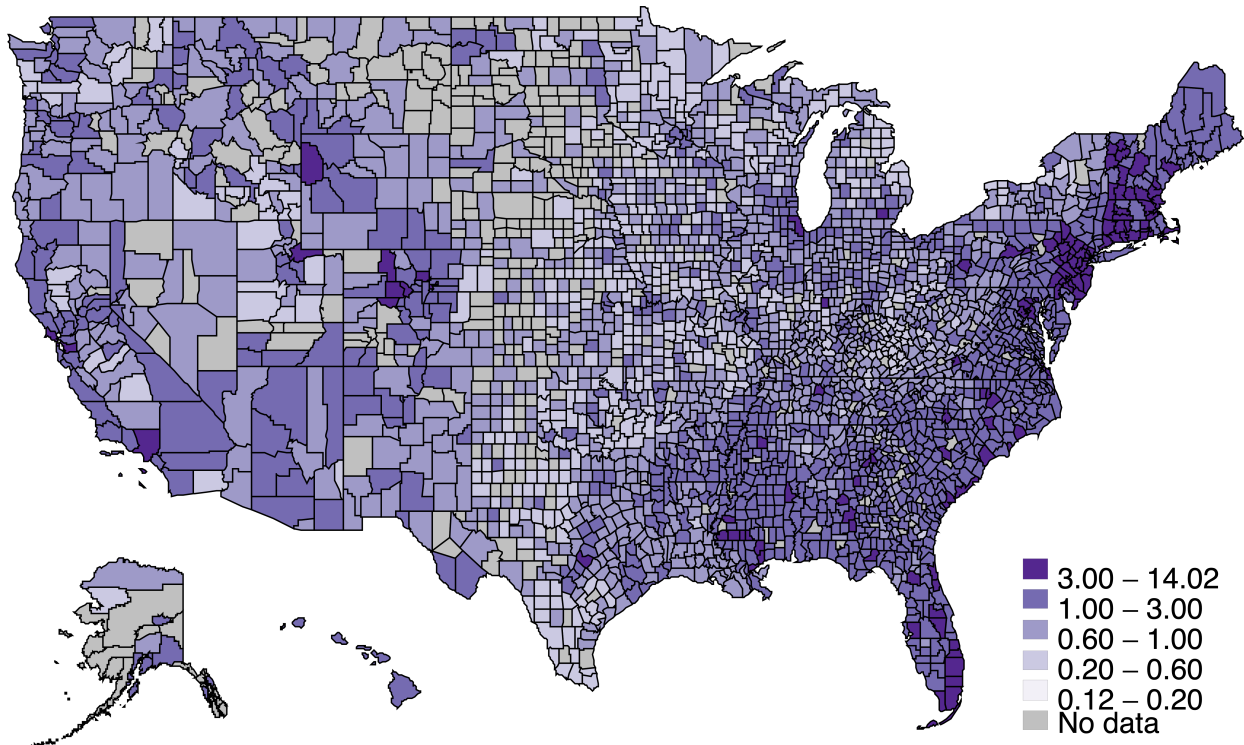
Notes.—Source: Facebook 2019 Social Connectedness Index (SCI). Panel A plots the number of COVID-19 infections per 1,000 individuals within each county as of April 1st, 2020. Panel B plots the SCI-weighted number of infections per 1,000 individuals, obtained by taking the population-weighted average across the product of infections in county c' and the SCI between county c and c' .

Figure A.2: Actual and Socially-connected COVID-19 Deaths

Nb of deaths per thousand (Apr 1st 2020)

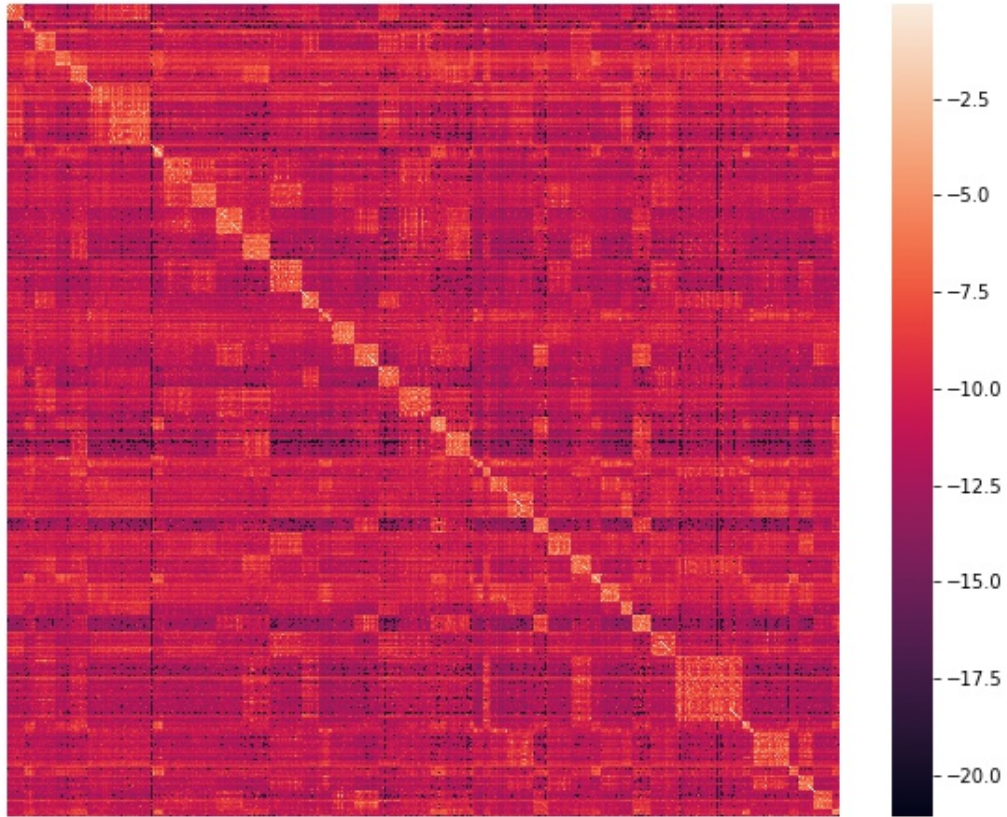


Nb of deaths per thousand on Facebook (Apr 1st 2020)



Notes.—Source: Facebook 2019 Social Connectedness Index (SCI). Panel A plots the number of COVID-19 deaths per 1,000 individuals within each county as of April 1st, 2020. Panel B plots the SCI-weighted number of deaths per 1,000 individuals, obtained by taking the population-weighted average across the product of deaths in county c' and the SCI between county c and c' .

Figure A.3: Listening Matrix Across Counties

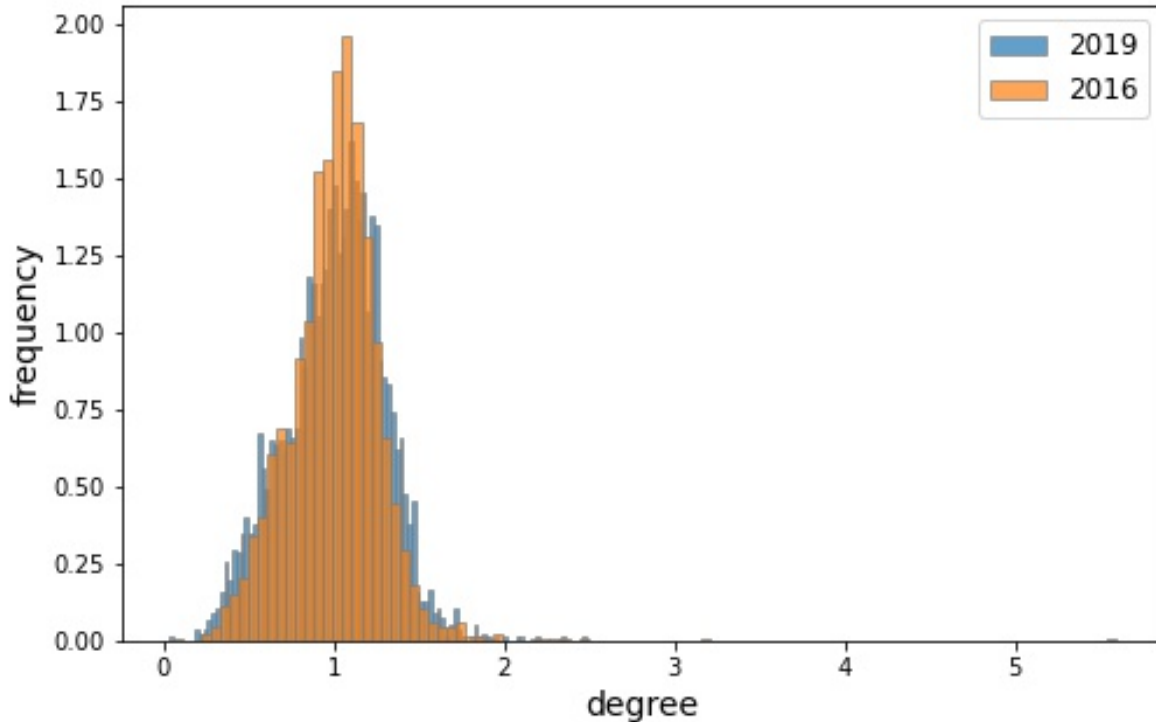


Notes.—Source: Facebook 2019 Social Connectedness Index (SCI). The heatmap plots the logged listening matrix of 3141 U.S. counties according to SCI data of 2019. The matrix W is defined as in Equation 3. The i -th row and j -th column entry of the W , $w_{i,j}$, represents the social influence the j -th node has on i -th node in the network.

network is 1. The observed standard deviation, a measure of the dispersion of influences, is 0.27 in 2016 and 0.29 in 2019, respectively. This suggests that social network connections have grown more dispersed over time. All symmetric matrices have the property that all nodes are of degree 1 thus zero-dispersion represents. In contrast, higher dispersion of the degrees implies the nodes have more asymmetric influences on others across the network. A more disperse distribution in 2019 compared to 2016 will lead to a higher degree of amplification of local shocks to the whole network albeit small in size, as we will see in the next sections. These differences across the network imply

that the aggregate fluctuations in consumption will depend on where the initial shocks take place.

Figure A.4: Distribution of the Degree of Direct Influences in the Network



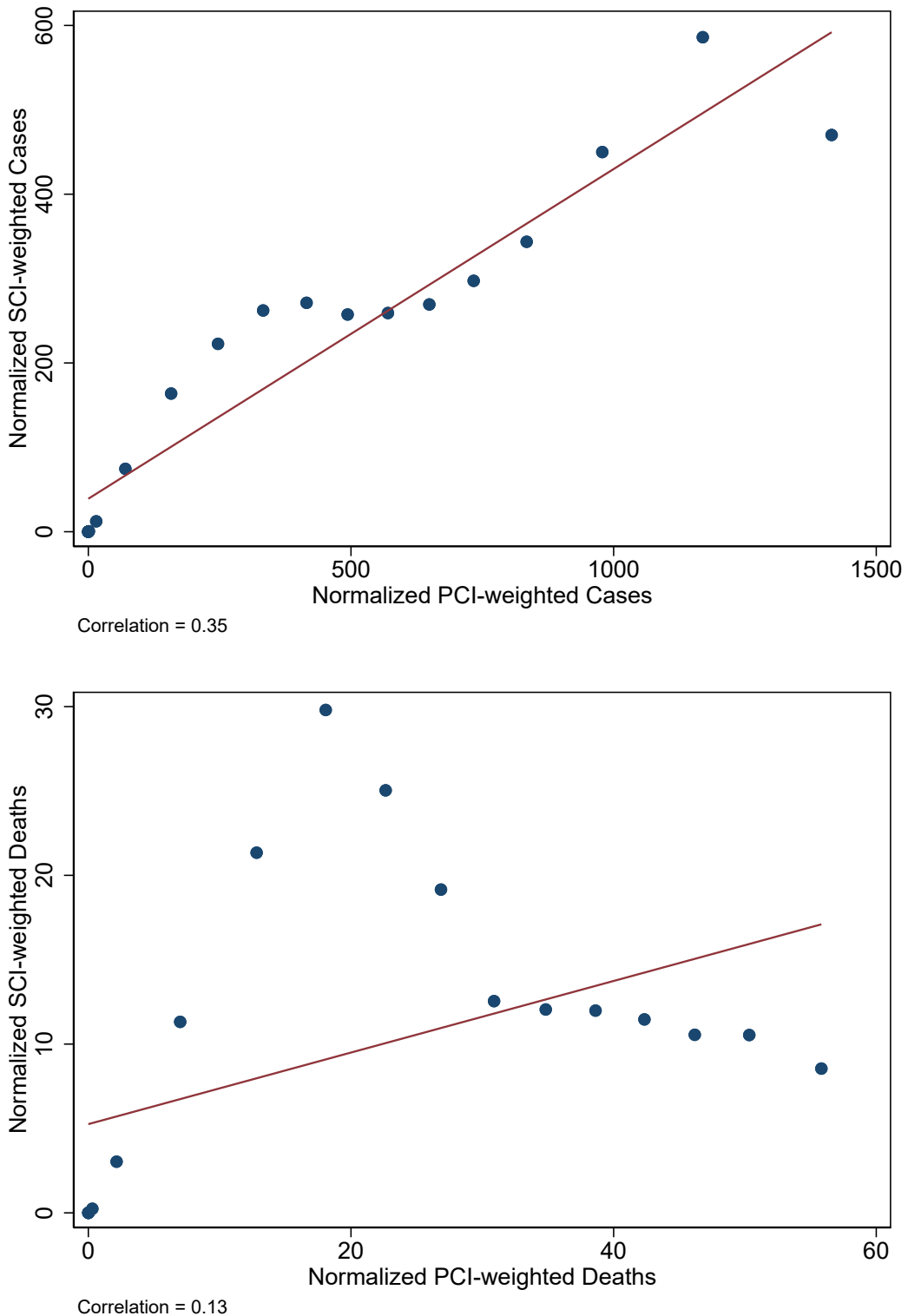
Notes.—Source: Facebook Social Connectedness Index (SCI) for 2016 and 2019. The histogram plots the distribution of degrees of 3141 counties according to SCI's 2016 and 2019 extracts, respectively. The degree is defined as in Equation 5.

A.3 Supplement to the Empirical Results

We now explore several robustness exercises to our main empirical results that show how increases in the number of SCI-weighted cases are associated with declines in consumption. One of our concerns is that social connectivity is simply a proxy for physical proximity. We examine this concern by obtaining the distance from each county to every other county, just as in our SCI data, and use it to construct a similar index for coronavirus cases, which we call the physical connectedness index (PCI). Figure A.5 documents these results, showing that there is only a correlation of 0.35 (0.13) between the SCI and PCI -weighted number of coronavirus cases (deaths). This suggests that social

connectivity is not simply capturing differences in physical distance.

Figure A.5: Social and Physical Connectedness -Weighted Coronavirus Cases & Deaths



Notes.—Sources: Facebook Social Connectedness Index and the NBER Physical Distance data. The figure documents the number of coronavirus cases and deaths constructed using the physical and social connectedness indices normalized to the total distance and number of friendship ties.

We subsequently investigate the role of physical distance in greater detail by replicating the main results under different specifications with physical distance as a control. Table A.1 documents these results. We present the simple specification in columns 1 and 5: a 10% rise in SCI-weighted cases and deaths is associated with a 0.5% and 0.16% decline in consumption expenditures. After we add PCI-weighted cases and deaths, our main results are not significantly altered: our coefficient on logged SCI-weighted cases is statistically indistinguishable and the coefficient on logged SCI-weighted deaths is even larger (columns 2 and 6). Columns 3 and 7 subsequently add time-varying state policy controls, which only reduces the magnitude of our coefficients marginally. Finally, columns 4 and 8 add two-week lagged values of logged coronavirus cases and deaths. Although the coefficients decline in magnitude, the main results remain statistically and economically significant. We also note that PCI-weighted cases is not associated with consumption, but PCI-weighted deaths is strongly negatively correlated with consumption.

In summary, these results show that our SCI-weighted coronavirus cases and deaths index is not simply capturing variation in physical distance. Moreover, even when we control explicitly for a comparable measure of PCI-weighted cases and deaths, our results remain. These exercises are on top of the baseline specification, which excludes counties in the same state (otherwise closely connected geographies).

Since our consumption data is based on a sample of debit-card users that is disproportionately represented by young and low-income people, it is also worth checking if the empirical results are robust to an alternative measure of consumer spending from separate data source. We utilize the county-level consumer spending of 1481 counties across the United States based on both debit and credit card transaction data provided by Affinity, a commercial provider.²⁰ Table A.2 reports the results of the same regression as the baseline except for replacing the dependent variable with the

²⁰Chetty et al. (2020) shows that the aggregate series of the transaction data tracks the national retail sales (excluding auto and gas) from the Monthly Retail Trade Survey remarkably well.

Table A.1: Examining the Role of Physical Distance for Predicting Consumption Responses

Dep. var. =	log(Consumption Expenditures)							
	(1)	(2)	(3)	(4)	(5)	(6)	(7)	(8)
log(SCI-weighted Cases)	-.051*** [.004]	-.050*** [.006]	-.042*** [.007]	-.017** [.008]				
log(SCI-weighted Deaths)					-.016** [.007]	-.050*** [.006]	-.046*** [.006]	-.023*** [.009]
log(PCI-weighted Cases)	.007 [.018]	.006 [.018]	.026 [.017]					
log(PCI-weighted Deaths)						-.175*** [.016]	-.175*** [.015]	-.157*** [.015]
log(County Cases), 14 day Lag				-.018*** [.004]				-.022*** [.004]
log(County Deaths), 14 day Lag				.008 [.006]				.011** [.005]
R-squared	.99	.99	.99	.99	.99	.99	.99	.99
Sample Size	351644	351644	351644	351644	351644	351644	351644	351644
County FE	Yes	Yes	Yes	Yes	Yes	Yes	Yes	Yes
Time FE	Yes	Yes	Yes	Yes	Yes	Yes	Yes	Yes
State Policies	No	No	Yes	Yes	No	No	Yes	Yes

Notes.—Sources: Facebook Social Connectedness Index (SCI) for 2019, Facteus. The table reports the coefficients associated with regressions of logged consumption spending on logged SCI and PCI -weighted infections (excluding county c 's friendship ties with itself) and logged county infections and deaths, conditional on county and time fixed effects. Consumption is deflated by the national personal consumption expenditure index. Our SCI-weighted cases and death index is constructed as follows: $COVID_{c,t}^{SCI} = \sum_{c'} (COVID_{c',t} \times SCI_{c,c'})$ where $COVID_{ct}^{SCI}$ denotes the logged SCI-weighted number of cases or deaths in connected counties, $COVID_{c',t}$ denotes the logged number of cases or deaths in county c' , and $SCI_{c,c'}$ denotes our measure of the SCI. We normalize the scaled number of friendship ties in a county to its total number of friendship ties, thereby exploiting the relative exposure to other locations. The physical connectedness index (PCI) is constructed similar using miles between counties, rather than friendship ties. Our variables that are denoted “other states” construct the SCI excluding counties within the same state to control for physical proximity. Standard errors are clustered at the county-level and observations are weighted by county population. The sample period is between March 1st to June 30th, 2020.

growth rate relative to January 2020 of each day. The negative and significant coefficients associated with the SIC weighted cases and deaths remain negative and significant.

Table A.2: Alternative Data Source of Consumption Spending

Dep. var. =	log(Consumption Expenditures) Growth							
	(1)	(2)	(3)	(4)	(5)	(6)	(7)	(8)
Has SAHO			-.011*** [.003]	.015** [.007]			-.010*** [.003]	-.008** [.003]
log(SCI-weighted Cases)	-.028*** [.004]	-.018*** [.005]	-.029*** [.004]	-.025*** [.004]				
× SAHO					-.008*** [.002]			
log(SCI-weighted Deaths)						-.023*** [.003]	-.024*** [.004]	-.042*** [.005]
× SAHO								-.004* [.002]
log(County Cases)	.000 [.002]	.002 [.002]	.002 [.002]			-.003* [.001]	-.001 [.001]	-.001 [.001]
log(County Deaths)	-.007*** [.003]	-.007*** [.001]	-.007*** [.001]			.003 [.002]	.001 [.002]	.001 [.002]
R-squared	.84	.84	.75	.75	.73	.73	.75	.75
Sample Size	175857	175857	175857	175857	175857	175857	175857	175857
County FE	Yes	Yes	Yes	Yes	Yes	Yes	Yes	Yes
Time FE	Yes	Yes	Yes	Yes	Yes	Yes	Yes	Yes
State Policies	No	No	Yes	Yes	No	No	Yes	Yes
State x Month FE	No	No	Yes	Yes	No	No	Yes	Yes

Notes.—Sources: Facebook Social Connectedness Index (SCI) for 2019, Affinity Solutions. The table reports the coefficients associated with regressions of logged consumption spending growth from January 1st on logged SCI-weighted infections and logged county infections and deaths, conditional on county and time fixed effects. The consumption spending is from the Affinity Solution, including both debit and credit card transactions of consumption spending at the county level.

A.4 Derivations and Proofs of Model Results

Steady state of the Kalman filtering

Under efficient updating using Kalman filtering, the weight $\kappa_{i,t}$ evolves as the following.

$$\kappa_{i,t} = \frac{\Sigma_{i,t-1}}{\Sigma_{i,t-1} + \sigma_\theta^2 + \sigma_\eta^2} \quad (24)$$

$$\Sigma_{i,t} = (1 - \kappa_{i,t})(\Sigma_{i,t-1} + \sigma_\theta^2)$$

where $\Sigma_{i,t-1}$ is i's prior uncertainty regarding ψ_t before updating.

Combining the two equations gives

$$\Sigma_{i,t} = \frac{\sigma_\theta^2 + \sigma_\eta^2}{\Sigma_{i,t-1} + \sigma_\theta^2 + \sigma_\eta^2} (\Sigma_{i,t-1} + \sigma_\theta^2) \quad (25)$$

In steady state, $\Sigma_{i,t} = \Sigma^* \quad \forall t$ and $\kappa_{i,t} = \kappa^* \quad \forall t$. We can solve it as

$$\kappa^* = \frac{\sqrt{(\sigma_\theta^2 + \sigma_\eta^2)\sigma_\theta^2}}{\sqrt{(\sigma_\theta^2 + \sigma_\eta^2)\sigma_\theta^2} + \sigma_\theta^2 + \sigma_\eta^2} \quad (26)$$

Evolution of average belief

We define the average belief of the society at time t by $\tilde{\psi}_t^{av}$ as following, where H is a $1 \times N$ vector and N is the number of agents in the economy.

$$\tilde{\psi}_t^{av} = \frac{1}{N} H \tilde{\psi}_t \quad (27)$$

Using the law of motion of the social belief from Equation 9, we can write v -step-ahead average belief $\tilde{\psi}_{t+v}^{av}$ as a function of realized signals between t and $t+v$ as the following.

$$\tilde{\psi}_{t+v}^{av} = \prod_{h=1}^v M_{t+h} \tilde{\psi}_t^{av} + \frac{1}{N} H \sum_{s=0}^v \prod_{h=1}^s M_{t+h} (1 - \lambda) \kappa_{t+s} s_{t+s} \quad (28)$$

Under constant-gain learning

Under constant-gain learning, we can drop the time script t from κ_t and further assume it to be a constant k across individuals, then κ_t becomes a constant diagonal matrix.

$$\kappa_t = kI \quad \forall t \quad (29)$$

Then time scripts in κ_t and M_t in the Equation 28 all drop.

$$\tilde{\psi}_{t+v}^{av} = M^v \tilde{\psi}_t^{av} + \frac{1}{N} H \sum_{s=0}^v M^s (1 - \lambda) k I s_{t+s} \quad (30)$$

Belief multiplier to exogenous local and aggregate belief shocks

Aggregate effect v periods after a shock to j 's belief

$$\begin{aligned} MP_{t+v|t}^j &= \frac{\overbrace{\delta \tilde{\psi}_{t+v}^{av} / \delta \tilde{\psi}_{j,t} (\lambda \neq 0)}^{\text{social effect+composition effect}}}{\underbrace{\delta \tilde{\psi}_{t+v}^{av} / \delta \tilde{\psi}_{j,t} (\lambda = 0)}_{\text{composition effect}}} \\ &= 1, \quad v = 0 \\ &= \left(\frac{d_j}{1-k} - 1 \right) \lambda + 1 > 1 \quad \text{if } d_j + k > 1, \quad v = 1 \\ &= \frac{\lambda^2}{(1-k)^2} \underbrace{\sum_{s=1}^N d_s w_{s,j}}_{\tilde{d}_j} + \frac{2(1-\lambda)\lambda}{1-k} d_j + (1-\lambda)^2, \quad v = 2 \\ &\dots \end{aligned}$$

where \tilde{d}_j is the friends-weighted influence (degree) of j . $\tilde{d}_j \uparrow$ as $d_j = \sum_{s=1}^N w_{s,j} \uparrow$ $\tilde{d}_j > d_j$ if $d_j > 1$

As a special case, let $\lambda = 1$, then we have

$$MP_{t+v|t}^j = \frac{1}{(1-k)^2} \sum_{s=1}^N d_s w_{s,j} > 1 \quad \text{if } \tilde{d}_j > (1-k)^2$$

The average belief v periods after an exogenous belief shock to all the nodes, the belief multiplier is equal to the sum of individual MP following each node, which is

$$\begin{aligned}
 \sum_{s=1}^N d_s &= N \rightarrow \\
 MP_{t+v|t} &= \frac{1}{N} \sum_{j=1}^N MP_{t+v|t}^j \\
 &= \frac{1}{N} N = 1, \quad v = 0 \\
 &= \frac{1}{N} \frac{\sum_{j=1}^N d_j}{1-k} \lambda + (1-\lambda) = \underbrace{\frac{1}{1-k} \lambda + (1-\lambda)}_{\Theta}, \quad v = 1 \\
 &= \frac{1}{N} \sum_{j=1}^N \tilde{d}_j = \frac{\lambda^2}{(1-k)^2} + \frac{2(1-\lambda)\lambda}{1-k} + (1-\lambda)^2 = \Theta^2, \quad v = 2 \\
 \text{for } \sum_{j=1}^N \tilde{d}_j &= \sum_{j=1}^N \sum_{s=1}^N d_s w_{s,j} = \sum_{s=1}^N d_s \sum_{j=1}^N w_{s,j} = N \\
 \dots
 \end{aligned} \tag{31}$$

Aggregate belief responses to the aggregate news

The news in our model s_t consists of one aggregate component and an idiosyncratic component which can be stacked up as η_t . The shock to the former, θ_t is permanent, while the latter plays the role of idiosyncratic and serially independent noises by the assumption of the paper.

$$s_t = \xi_t - \xi_{t-1} = \psi_t H' + \eta_t = \psi_{t-1} H' + \theta_t H' + \eta_t \tag{32}$$

Notice the aggregate shock θ_t enters the news permanently, i.e. there is θ_t in s_t, s_{t+1}, \dots . Therefore, the v -step impulse response(IRF) of average belief to θ_t can be summarized by the following scalar.

$$\begin{aligned}
\widetilde{IRF}_{t+v}^{ag} &= \frac{\delta \tilde{\psi}_{t+v}^{av}}{\delta \theta_t} = \frac{1}{N}(1-\lambda)kH \sum_{s=0}^v M^s H' \quad \forall v = 0, 1, \dots \\
&= \frac{1}{N}(1-\lambda)k \sum_{s=0}^v \sum_i^N \sum_j^N m_{i,j}^s
\end{aligned} \tag{33}$$

where $m_{i,j}^s$ is the i,j entry of the matrix M to the power of s . Combining the fact that $\sum_i^N \sum_j^N w_{i,t} = N$, we can show the following.

$$\begin{aligned}
\widetilde{IRF}_{t+v}^{ag} &= \sum_{s=0}^v x^s \\
x^s &= (1-\lambda)k[(1-\lambda)(1-k) + \lambda]^s
\end{aligned} \tag{34}$$

In general, the IRF is a function of λ , k , and the time horizon v . Critically, it does not depend on the network structure W . A trivial case is when $v = 0$, $\widetilde{IRF}_t^{ag} = (1-\lambda)k$, increasing in k and decreasing in λ . This does not depend on W since social communication has not incorporated the newly updated private belief. From $v = 1$ onward, the repeated social communications start propagating these beliefs across society.

Aggregate belief response to local news

Similarly, we can define impulse response of average belief to a vector of shocks to the η_t . But the difficulty is that since the response will depend on many details such as the size and the exact locations of each node-specific shock, we cannot derive a close-form formula of IRF for a general $N \times 1$ vector of the shocks.

To proceed, we focus on a special case. If the imagined shock is an equal-sized shock of $\underline{\eta}_t$ (a scalar) in all the nodes whose influence measured by degree is above a cutoff level \underline{d} . We can more specifically rewrite the shock to η_t as $\underline{\eta}_t Z_t$ where

$$Z_t = [\mathbb{1}(1 \in \Omega), \mathbb{1}(2 \in \Omega), \dots, \mathbb{1}(N \in \Omega)]' \quad (35)$$

$$\Omega = \{i \in \{1, 2, \dots, N\} | d_i \geq \underline{d}\}$$

Combining Equation 32, we can then derive the v step impulse response for this special with respect to $\underline{\eta}_t$ as below.

$$\widetilde{IRF}_{t+v}^{id'} = \frac{\delta \tilde{\psi}_{t+v}^{av}}{\delta \underline{\eta}_t} = \frac{1}{N}(1 - \lambda)kHM^v Z_t \quad \forall v = 0, 1, \dots \quad (36)$$

A special case when $v = 0$, $\widetilde{IRF}_t^{id'} = \frac{1}{N}(1 - \lambda)k \sum_{i=1}^N \mathbb{1}(i \in \Omega)$ and it decreases in both λ and k .

The actual v -step-ahead IRF of the ψ_{t+v} to the aggregate shock θ_t is exactly 1. The difference between $\widetilde{IRF}_{t+v}^{ag}$ and 1 characterizes the belief deviation or nowcasting error of the society.

Since all the shocks are idiosyncratic and transitory and the aggregate state ψ_t stays the same, the actual IRF in all horizons is zero. The difference between $\widetilde{IRF}_{t+v}^{id'}$ and zero characterizes social belief deviation from the local shocks.

References

- Acemoglu, D., Carvalho, V. M., Ozdaglar, A., and Tahbaz-Salehi, A. (2012). The network origins of aggregate fluctuations. *Econometrica*, 80(5):1977–2016.
- Acemoglu, D., Ozdaglar, A., and ParandehGheibi, A. (2010). Spread of (mis) information in social networks. *Games and Economic Behavior*, 70(2):194–227.
- Agarwal, S., Liu, C., and Souleles, N. S. (2007). The reaction of consumer spending and debt to tax rebates: Evidence from consumer credit data. *Journal of Political Economy*, 115(6):986–1019.

- Aguiar, M. and Bils, M. (2015). Has consumption inequality mirrored income inequality? *American Economic Review*, 105(9):2725–56.
- Aguiar, M. and Hurst, E. (2013). Deconstructing life cycle expenditure. *Journal of Political Economy*, 121(3):437–492.
- Ali, U., Herbst, C. M., and Makridis, C. A. (2021). The Impact of Covid-19 on the U.S. Child Care Market: Evidence from Stay-at-Home Orders. *Economics of Education Review*, 82.
- Attanasio, O. P. and Pistaferri, L. (2016). Consumption inequality. *Journal of Economic Perspectives*, 30(2):3–28.
- Bailey, M., Cao, R., Kuchler, T., and Stroebel, J. (2018a). The economic effects of social networks: Evidence from the housing market. *Journal of Political Economy*, 126(6):2224–2276.
- Bailey, M., Cao, R., Kuchler, T., and Stroebel, J. (2018b). The economic effects of social networks: Evidence from the housing market. *Journal of Political Economy*, 126(6):2224–2276.
- Bailey, M., Cao, R., Kuchler, T., Stroebel, J., and Wong, A. (2018c). Social connectedness: Measurement, determinants, and effects. *Journal of Economic Perspectives*, 32(3):259–280.
- Baker, S. R., Bloom, N., Davis, S. J., and Terry, S. J. (2020a). COVID-induced economic uncertainty. *NBER working paper*.
- Baker, S. R., Farrokhnia, R. A., Meyer, S., Pagel, M., and Yannelis, C. (2020b). How Does Household Spending Respond to an Epidemic? Consumption During the 2020 COVID-19 Pandemic. *Working paper*.
- Baqae, D. R. and Farhi, E. (2018). Macroeconomics with heterogeneous agents and input-output networks. Technical report, National Bureau of Economic Research.

- Bartik, A. W., Betrand, M., Lin, F., Rothstein, J., and Unrath, M. (2020). Labor market impacts of COVID-19 on hourly workers in small- and medium- size businesses: Four facts from HomeBase data. *Chicago Booth Rustandy Center, Working Paper*.
- Bayer, P., Mangum, K., and Roberts, J. W. (2021). Speculative fever: Investor contagion in the housing bubble. *American Economic Review*, 111(2):609–51.
- Binder, C. and Makridis, C. A. (2020). Stuck in the Seventies: Gas Prices and Macroeconomic Expectation. *Review of Economics & Statistics, R&R*.
- Blundell, R., Pistaferri, L., and Preston, I. (2008). Consumption inequality and partial insurance. *American Economic Review*, 98(5):1887–1921.
- Bordalo, P., Gennaioli, N., Ma, Y., and Shleifer, A. (2020). Overreaction in macroeconomic expectations. *American Economic Review*.
- Burnside, C., Eichenbaum, M., and Rebelo, S. (2016). Understanding booms and busts in housing markets. *Journal of Political Economy*, 124(4):1088–1147.
- Bursztyn, L., Ederer, F., Ferman, B., and Yucghtman, N. (2014). Understanding mechanisms underlying peer effects: Evidence from a field experiment. *Econometrica*, 82(4):1273–1301.
- Cajner, T., Crane, L., Decker, R. A., Grigsby, J., Hamins-Puertolas, A., Hurst, E., Kurz, C., and Yildirmaz, A. (2020). The U.S. labor market during the beginning of the pandemic recession. *BFI working paper*.
- Carroll, C., Slacalek, J., Tokuoka, K., and White, M. N. (2017). The distribution of wealth and the marginal propensity to consume. *Quantitative Economics*, 8(3):977–1020.

- Carroll, C. D. (2003). Macroeconomic Expectations of Households and Professional Forecasters. *Quarterly Journal of Economics*, 118(1):269–298.
- Carroll, C. D. (2011). Solution methods for microeconomic dynamic stochastic optimization problems. *World Wide Web*: <http://www.econ.jhu.edu/people/ccarroll/solvingmicrodsops.pdf>. (accessed August 30, 2011). Cited on, page 28.
- Carroll, C. D., Fuhrer, J. C., and Wilcox, D. W. (1994). Does consumer sentiment forecast household spending? If so, why? *American Economic Review*, 84(5):1397–1408.
- Castaneda, A., Diaz-Gimenez, J., and Rios-Rull, J.-V. (2003). Accounting for the us earnings and wealth inequality. *Journal of political economy*, 111(4):818–857.
- Chandrasekhar, A. G., Larreguy, H., and Xandri, J. P. (2020). Testing models of social learning on networks: Evidence from two experiments. *Econometrica*, 88(1):1–32.
- Charoenwong, B., Kwan, A., and Pursiainen, V. (2020). Social connections with COVID-19 affected areas increase compliance with mobility restrictions. *Working paper*.
- Chen, X., Hong, H., and Nekipelov, D. (2011). Nonlinear models of measurement errors. *Journal of Economic Literature*, 49(4):901–937.
- Chetty, R., Friedman, J. N., Hendren, N., Stepner, M., et al. (2020). How did covid-19 and stabilization policies affect spending and employment? a new real-time economic tracker based on private sector data. Technical report, National Bureau of Economic Research.
- Cogley, T. and Sargent, T. J. (2008). The market price of risk and the equity premium: A legacy of the Great Depression. *Journal of Monetary Economics*, 55(3):454–476.

- Coibion, O. and Gorodnichenko, Y. (2015a). Information rigidity and the expectations formation process: A simple framework and new facts. *American Economic Review*, 105(8):2644–78.
- Coibion, O. and Gorodnichenko, Y. (2015b). Information Rigidity and the Expectations Formation Process: A Simple Framework and New Facts. *American Economic Review*, 105(8):2644–2678.
- Coibion, O., Gorodnichenko, Y., and Weber, M. (2020a). Labor markets during the COVID-19 crisis: A preliminary view. *NBER working paper*.
- Coibion, O., Gorodnichenko, Y., and Weber, M. (2020b). The cost of the COVID-19 crisis: Lock-downs, macroeconomic expectations, and consumer spending. *NBER working paper*.
- De Giorgi, G., Frederiksen, A., and Pistaferri, L. (2020). Consumption network effects. *The Review of Economic Studies*, 87(1):130–163.
- DeGroot, M. H. (1974). Reaching a consensus. *Journal of the American Statistical Association*, 69(345):118–121.
- DeMarzo, P. M., Vayanos, D., and Zwiebel, J. (2003). Persuasion bias, social influence, and unidimensional opinions. *Quarterly Journal of Economics*, 118(3):909–968.
- Di Maggio, M., Kermani, A., Keys, B. J., Piskorski, T., Ramcharan, R., Seru, A., and Yao, V. (2017). Interest rate pass-through: Mortgage rates, household consumption, and voluntary deleveraging. *American Economic Review*, 107(11):3550–3588.
- Dingel, J. I. and Neiman, B. (2020). How many jobs can be done at home. *BFI working paper*.
- Eichenbaum, M., Rebelo, S., and Trabandt, M. (2020). The macroeconomics of epidemics. *NBER working paper*.

- Friedkin, N. E. and Johnsen, E. D. (1999). Social influence networks and opinion chance. *Advances in Group Processes*, 16:1–29.
- Fuster, A., Kaplan, G., and Zafar, B. (2018). Wht would you do with \$500? Spending responses to gains, losses, news and loans. *NBER working paper*, Review of Economic Studies, R&R.
- Gallipoli, G. and Makridis, C. (2018). Structural Transformation and the Rise of Information Technology. *Journal of Monetary Economics*, 97:91–110.
- Gillitzer, C. and Prasad, N. (2018). The effect of consumer sentiment on consumption: Cross-sectional evidence from elections. *American Economic Journal: Macroeconomics*, 10(4):234–269.
- Giuliano, P. and Spilimbergo, A. (2014). Growing up in a Recession. *Review of Economic Studies*, 81(2):787–817.
- Goldsmith-Pinkham, P. and Imbens, G. W. (2013). Social Networks and the Identification of Peer Effects. *Journal of Business & Economic Statistics*, 31(3):253–264.
- Golub, B. and Jackson, M. O. (2010). Naive learning in social networks and the wisdom of crowds. *American Economic Journal: Microeconomics*, 2(1):112–49.
- Gourinchas, P.-O. and Parker, J. A. (2002). Consumption over the life cycle. *Econometrica*, 70(1):47–89.
- Guerrieri, V., Lorenzoni, G., Straub, L., and Werning, I. (2020). Macroeconomic Implications of COVID-19: Can Negative Supply Shocks Cause Demand Shortages? *NBER working paper*.
- Heathcote, J., Perri, F., and Violante, G. L. (2010). Unequal we stand: An empirical analysis of economic inequality in the United States, 1967-2006. *Review of Economic Dynamics*, 13:15–51.

- Heathcote, J., Storesletten, K., and Violante, G. L. (2014). Consumption and labor supply with partial insurance: An analytical framework. *American Economic Review*, 104(7):1–52.
- Heffetz, O. (2011). A test of conspicuous consumption: Visibility and income elasticities. *Review of Economics and Statistics*, 93(4):1101–1117.
- Jappelli, T. and Pistaferri, L. (2010). The consumption response to income changes. *Annual Review of Economics*, 2:479–506.
- Johnson, D. S., Parker, J. A., and Souleles, N. S. (2006). Household expenditure and the income tax rebates of 2001. *American Economic Review*, 96(5):1589–1610.
- Kaplan, G. and Violante, G. L. (2010). How much consumption insurance beyond self-insurance. *American Economic Journal: Macroeconomics*, 2(4):53–87.
- Kaplan, G. and Violante, G. L. (2014). A model of the consumption response to fiscal stimulus payments. *Econometrica*, 82(4):1199–1239.
- Krueger, D., Uhlig, H., and Xie, T. (2020). Macroeconomic dynamics and reallocation in an epidemic. *NBER working paper*.
- Kuchler, T. and Zafar, B. (2019). Personal experiences and expectations about aggregate outcomes. *Journal of Finance*, 74(5):2491–2542.
- Lehn, C. v. and Winberry, T. (2019). The investment network, sectoral comovement, and the changing us business cycle. Technical report, National Bureau of Economic Research.
- Makridis, C. (2020). The Effect of Economic Sentiment on Consumption: Evidence from Social Networks. *SSRN working paper*.

- Makridis, C. A. and Hartley, J. (2020). The cost of COVID-19: A rough estimate of the 2020 GDP impact. *Mercatus Center, Policy Brief Special Edition*.
- Makridis, C. A. and McGuire, E. (2020). Refined by Fire: The Great Depression and Entrepreneurship. *Working paper*.
- Malmendier, U. and Nagel, S. (2011). Depression babies: Do macroeconomic experiences affect risk taking? *Quarterly Journal of Economics*, 126(1):373–416.
- Malmendier, U. and Nagel, S. (2016). Learning from inflation experiences. *Quarterly Journal of Economics*, 131(1):53–87.
- Malmendier, U., Pouzo, D., and Vanasco, V. (2018). Investor experiences and financial market dynamics. *NBER Working Paper 24697*.
- Malmendier, U. and Shen, L. S. (2018). Scarred consumption. *NBER working paper*.
- Manski, C. F. (1993). Identification of endogenous social effects: The reflection problem. *The review of economic studies*, 60(3):531–542.
- Manski, C. F. (2000). Economic analysis of social interactions. *Journal of economic perspectives*, 14(3):115–136.
- Moretti, E. (2011). Social learning and peer effects in consumption: Evidence from movie sales. *Review of Economic Studies*, 78(1):356–393.
- Pistaferri, L. (2001). Superior information, income shocks, and the permanent income hypothesis. *Review of Economics and Statistics*, 83(3):465–476.
- Ritter, Z. (2020). Americans Use Social Media for COVID-19 Info, Connection. *Gallup*.

- Smith, A. and Anderson, M. (2018). Social media use in 2018. *Pew Center.*
- Souleles, N. S. (1999). The response of household consumption to income tax refunds. *American Economic Review*, 89(4):947–958.
- Ugander, J., Karrer, B., Backstrom, L., and Marlow, C. (2011). The anatomy of the facebook social graph. *arXiv preprint arXiv:1111.4503*.
- vom Lehn, C. and Winberry, T. (2020). The investment network, sectoral comovement, and the changing U.S. business cycle. *Quarterly Journal of Economics, R&R.*
- Westerman, D., Spence, P. R., and Van Der Heide, B. (2014). Social media as information source: Recency of updates and credibility of information. *Journal of Computer-Mediated Communication*, 19(2):171–183.
- Zeldes, S. P. (1989). Consumption and liquidity constraints: An empirical investigation. *Journal of Political Economy*, 97(2):305–346.